

Part 3—Forecasting Abundance of Walleye Pollock: Indices for Juvenile Abundance

RESULTS FROM THE INDICES WORKING GROUP: DEVELOPMENT AND APPLICATION TO FISHERY MANAGEMENT AND ECOSYSTEM INFORMATION ISSUES OF ENVIRONMENTAL INDICES IN THE EASTERN BERING SEA

Principal Authors: J.D. Schumacher and S.A. Macklin

With participation and contributions from the Indices Working Group:

Kerim Aydin, Nick Bond, Cathy Ferrar, Al Hermann, Anne Hollowed, Jim Ianelli, Nancy Kachel, Carol Ladd, Pat Livingston, Allen Macklin, Bern Megrey, Jeff Napp, Ron Reed, Dylan Righi, Sigrid Salo, Jim Schumacher, Alan Springer, Phyllis Stabeno, Peggy Sullivan, Terry Whitledge, and Tom Wilderbuer

3.1 Introduction

The goal of the Southeast Bering Sea Carrying Capacity program was to document the role of juvenile pollock in the eastern Bering Sea ecosystem. This included examination of factors that affect their survival and development and testing of annual indices of pre-recruit (age-1) abundance (SEBSCC, 1995). Within this framework, the purpose of the Indices Working Group (IWG, which was developed at the SEBSCC Principal Investigators meeting held in January 2001; membership as listed above) was defined as follows. Based on the best understanding of ecosystem dynamics, identify potential single- or multi-parameter constructs or indices (e.g., wind mixing, time of spring bloom, etc.) that lead to development of survival indices for pollock in the egg, larval, and young-of-the-year life history stages. Further, this information will provide input to the National Marine Fisheries Service (NMFS) stock assessment model and/or models of juvenile pollock for use by fisheries scientists at the Alaska Fisheries Science Center (AFSC)/NMFS and others interested in changes in the ecosystem.

In Section 3.2, we first present the conceptual framework for development of indices, including discussion of the time series of estimates of age-1 pollock recruitment (Fig. 3.1), which provides a base time series that indices can be evaluated against. Section 3.3 contains contributions from IWG members regarding development of potential indices (Table 3.1). Using a one-dimensional mixed layer model, Ladd and Stabeno (Section 3.3.1) developed an index of stratification. Stratification can influence larval and juvenile pollock survival through its impact on nutrient limitation, temperature and its inherent effects on physiological processes of the pollock and of their zooplankton prey. Megrey and Bond (Section 3.3.2) examine the potential impact of wind speed, a surrogate for mixing, as it might affect the ability of pollock larvae to feed. Napp and Kachel (Section 3.3.3) present time series of average net short wave radiation that has a direct impact on the timing of the spring phytoplankton bloom. This, in turn, has ramifications throughout the entire ecosystem (Hunt *et al.*, 2002a) and thus serves managers of components of this ecosystem by providing an index of the status and po-

Table 3.1: Environmental indices described in Section 3.3.

Index		1996	1997	1998	1999	2000	2001	2002
Wind Mixing								
	Low	0.35	0.61	0.35	0.35	0.45	0.42	0.26
	Optimum	0.65	0.26	0.58	0.61	0.42	0.58	0.55
	High	0.00	0.13	0.06	0.03	0.13	0.00	0.19
Stratification								
	Maximum	0.692	0.855	0.770	0.679	0.677	0.709	0.852
	Date	May 17	ice bloom	June 16	ice bloom	May 19	May 15	June 4
	Mixing Events	6	1	1	0	3	0	1
	Temperature	1.6	ice bloom	2.9	ice bloom	1.0	1.9	2.5
Light								
	[60°N, 170°W]	-150.3	-153.9	-141.2	-143.1	-145.5	-152.9	#N/A
	[57.5°N, 165°W]	-180.6	-196.3	-176.2	-187.1	-187.0	-188.7	#N/A
	[58°N, 159°W]	-185.0	-188.6	-175.3	-168.5	-181.0	-180.3	#N/A
Sea Ice								
		0.012	0.466	0.002	0.346	0.055	#N/A	#N/A
Cold Pool								
	T1	1.9	7.3	3.2	6.3	2.1	#N/A	#N/A
	T2	1.0	5.3	0.0	16.8	8.9	#N/A	#N/A
Advection								
		#N/A	0.059	0.003	0.000	0.045	0.003	#N/A
Age-0 Index								
		2.68	0.14	0.75	1.13	#N/A	#N/A	#N/A
Age-1 Abundance								
		26.6	42.3	17.5	17.5	24.5	25.7	11.1

Explanation of Indices

Wind Mixing: Fraction of period May 15 to June 15 when daily average surface wind speed (m s^{-1}) was <4.8 (low), 4.8–9.5 (optimum), >9.5 (high). [Estimated from NCEP winds.]

1-D Mixed Layer Model:

Stratification: Maximum (May–June) modeled stratification ($^{\circ}\text{C m}^{-1}$) (3-y running mean).

Date: When maximum stratification occurred.

Mixing Events: Number of times between stratification setup date and August 31 that modeled 3-day smoothed mixed layer depth increased >5 m in a day.

Temperature: Mixed layer temperature at max stratification date.

Light: Average net shortwave radiation (W m^{-2}) from April 1 through June 30 at [60°N, 170°W], [57.5°N, 165°W], and [58°N, 159°W] [from NCAR/NCEP Reanalysis].

Sea Ice: Average per cent concentration of sea ice within the region bounded by [58°N, 170°W] and [57°N, 165°W] during the period 15 March to 15 April.

Cold Pool: Estimated vertical areal slice of cold pool ($<2^{\circ}\text{C}$) water (km^2) contained along transect (on T1 during 1996 and 1999, the cold pool continued into shallower water).

Advection: Fraction of 735 simulated drifters that arrived after 90 days in the region between 57°–58°N and 165°–170°W.

Age-0 Index: Young-of-the-year abundance estimate (arbitrary units) from independent Pribilof survey.

Age-1 Abundance: Abundance estimates of 1-year old eastern Bering Sea pollock (billions) from Model 1 [2002 Stock Assessment].

tential trends in ecosystem structure. Sea ice influences the ecosystem via bottom-up (e.g., timing of peak phytoplankton production) and top-down (e.g., habitat) impacts. Salo and Stabeno (Section 3.3.4) developed time series of sea ice concentrations in various strata that establish the existence of strong spatial and interannual patterns. Because the extent and timing of sea ice largely determine the extent and yearly thermal characteristics of the cold pool, Sullivan (Section 3.3.5) developed time histories of water column temperature from the annual bottom trawl survey. These provide a different and more direct measure of the thermal field than does the sea ice index. The extent and magnitude of the cold pool may have implications for the distribution of adult pollock and hence cannibalism on young of the year fish (Wylie-Echeverria and Ohtani, 1999; Wylie-Echeverria, 1996; Wylie-Echeverria and Wooster, 1998). In Section 3.3.6, Ianelli considers using the estimated abundance of age-0 pollock from the Pribilof Islands area of the annual stock assessment as an index for juvenile pollock abundance. Hermann (Section 3.3.7) then provides a description of the Northeast Pacific Regional Ocean Modeling System (NEPROMS), as hydrodynamic model simulations can provide underpinning for the development of various indices. Righi (Section 3.3.7) presents an application of NEPROMS to the transport of pollock eggs and larvae. The connection to survival in these scenarios is the extent of overlap between the transported animals and older cannibalistic pollock. Importantly, the transport trajectories from the simulations more closely simulate actual conditions over the shelf than those used by Wespestad *et al.* (2000) in their examination of year-class success of pollock. Macklin (Section 3.3.8) presents a framework for cataloging indices.

Ianelli (Section 3.4) demonstrates how an index of early life history success is being used by NMFS for annual stock assessments. He presents an index of separation between juvenile and adult fish. Importantly, he points out that variation in location and timing of spawn, as well as the location in the water column of eggs and larvae must be accounted for in the development of more robust transport- and cannibalism-related indices. Springer (Section 3.5) examines changing relationships between climate and biological indices throughout the eastern Bering Sea, implying that different relationships likely apply during different phases of the climate regime. These results demonstrate the potential for using environmental indices (e.g., selected sea surface temperatures) as measures of ecosystem trends. Section 3.6 contains a synthesis of results from indices development and provides a road map for future development of indices. Section 3.6.3 presents concluding remarks that call for the development of informational products from the NEPROMS oceanographic model that would permit access to various model products by resource managers and users.

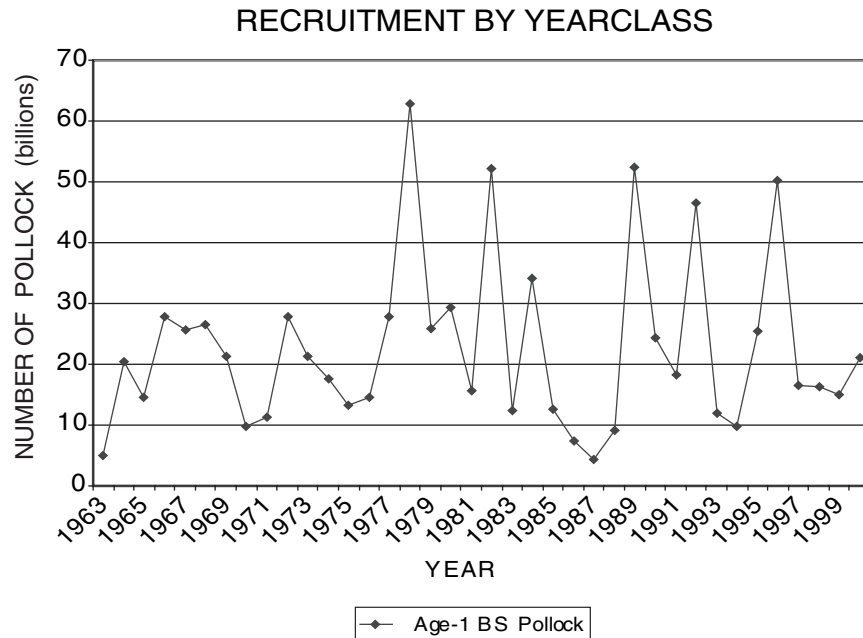


Figure 3.1: Recruitment of age-1 pollock in the eastern Bering Sea estimated as number of fish (from SAFE Report, 2001).

3.2 Conceptual Framework for Development of Indices

3.2.1 A pollock-centric perspective of the southeastern Bering Sea ecosystem

As noted by Napp *et al.* (2000), pollock is the most abundant species harvested in the Bering Sea, accounting for >65% of the total groundfish biomass during the 1980s when the total biomass exceeded 20 million tons. The biomass trends of three major trophic guilds in the eastern Bering Sea from 1979 to 1998 (Schumacher *et al.*, 2003) show that while the total biomass of pollock in the 1990s is less than in the 1980s, they still dominate biomass in any of the guilds which include marine birds, mammals, other fishes, and crabs. Walleye pollock is a nodal species in the food web (NRC, 1996) with juveniles being the dominant prey of fishes, seabirds, and marine mammals (Springer and Byrd, 1989; Livingston, 1993; Brodeur *et al.*, 1996). It is natural that pollock have been the focus of the Coastal Ocean Program's SEBSCC. The choice of developing a survival index for the early life history stages (eggs through young of the year) allows an early forecast of potential recruitment to the fishery and a metric that can be compared to existing time series of age-1 abundance (Fig. 3.1).

A switch model was developed for survival of pollock in the eastern Bering Sea (Megrey *et al.*, 1996). The model identifies candidates for cause of mortality by life history stage, the mortality variability of each stage, and indication of the stage contributing the most variability in recruitment to the fishery (Fig. 3.2). In this model, transport and turbulence have their greatest

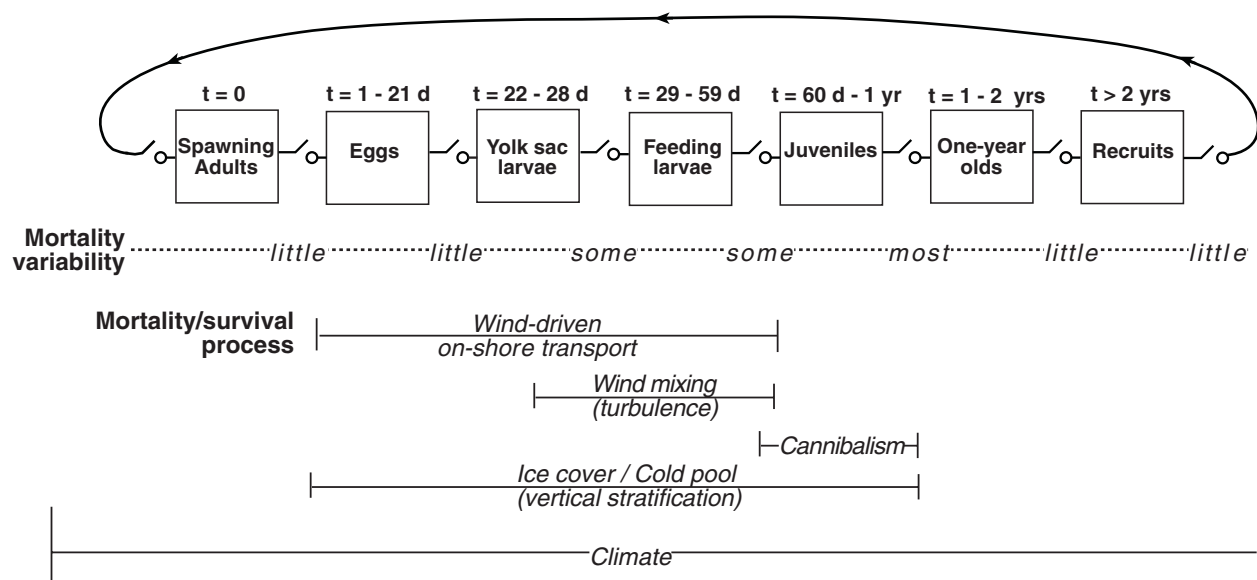


Figure 3.2: Switch model of pollock dynamics in the eastern Bering Sea. Processes thought to be important regulators of survival variability are shown and the span of their interaction is indicated.

impact on mortality of yoke-sack through feeding larval stages. It is the vertical structure and horizontal distribution of temperature, however, through their suggested influence on cannibalism, that have the greatest impact on recruitment (see Section 3.4 for more detail on egg/larval transport and the subsequent potential impact on cannibalism).

In a later version of the switch model, Napp *et al.* (2000) augmented the candidates that regulate survival by adding the timing of preferred prey production and the absence or presence of ice over the shelf region. Most recently, these have been woven together with other environmental factors to develop the Oscillating Control Hypothesis (OCH, Section 2.5), which examines how energy flow through the ecosystem may vary in different climate regimes (Hunt *et al.*, 2002a).

3.2.2 A generic model of pathways of energy flow through the ecosystem

Although the focus on pollock is reasonable, and models that have pollock as the central feature helped focus research in SEBSCC, a more inclusive perspective also has value. This is particularly true when considering questions on the ecosystem scale, e.g., the dramatic decline in abundance of the Steller sea lion. Identifying and understanding mechanisms that transfer climate change via the ocean to biota is essential if we are to understand ecosystem dynamics (Francis *et al.*, 1998). Fluctuations in the physical environment can impact the ecosystem through both changes in the nutrient-phytoplankton-zooplankton sequence (i.e., bottom-up control), and/or by altering habitat resulting in changes in abundance and/or composition of higher trophic level animals (i.e., top-down control). Hunt *et al.* (2002a) hy-

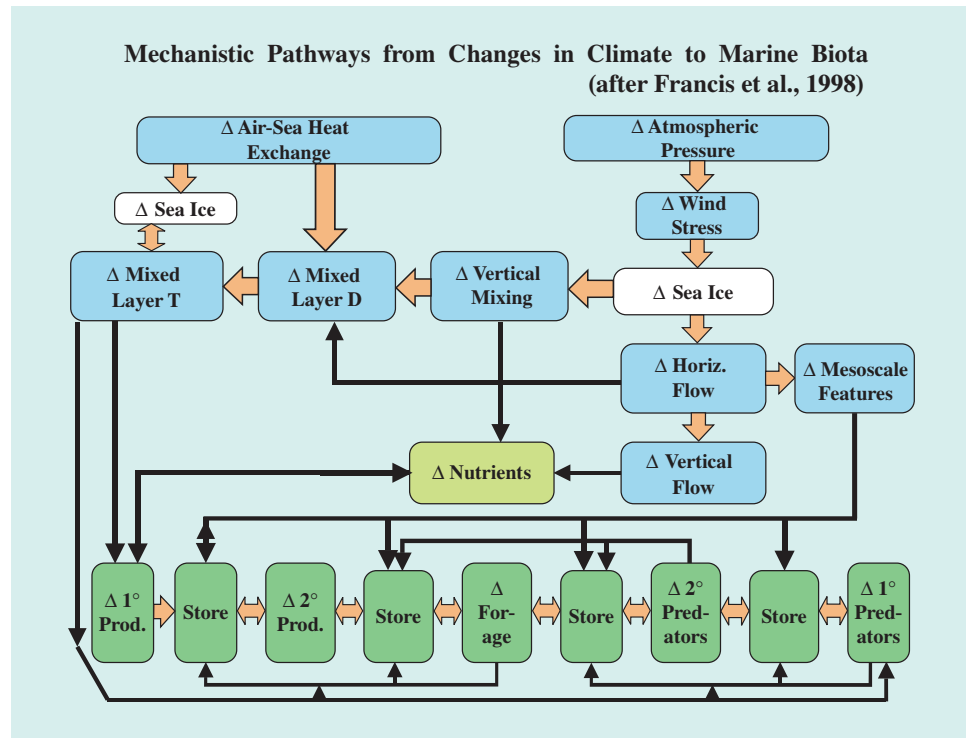


Figure 3.3: Conceptual model showing the pathways through which changes in atmospheric features can influence oceanic and biological components of the ecosystem of the eastern Bering Sea (from Schumacher *et al.*, 2003).

pothesize that the control of energy flow on the shelf (either top down or bottom up) depends on the timing of the nutrient-phytoplankton-zooplankton sequence related to the presence/absence of sea ice.

More inclusive and general conceptual models have been developed for the eastern Bering Sea and North Pacific Ocean. Schumacher *et al.* (2003) adapted the Francis *et al.* (1998) conceptual model of the pathways by which climate phenomena influence the biota to include sea ice, a dominant feature of the ecosystem of the eastern Bering Sea shelf (Fig. 3.3).

This model shows that there are numerous ecosystem elements (Section 3.5 discusses relationships between adjacent and more widely separated ecosystem elements) and connecting processes to consider when attempting to understand the impact of changes in atmospheric pressure on survival of young pollock. For example, a change in characteristics of the Aleutian Low will alter wind stress and the ensuing horizontal flow field (upper layer currents). It also will impact vertical mixing and air-sea heat fluxes and, thereby, the temperature of the upper mixed layer. These changes in transport, turbulence and temperature can impact the biological ecosystem element of interest either by enhancing or limiting survival, or both.

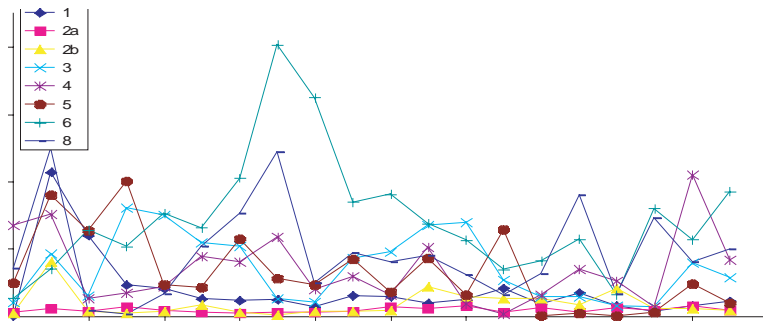


Figure 3.4: Abundance of adult pollock in the unequal areas used in the development of the ice index (Section 4.3.4).

3.2.3 Other aspects of indices development

As expected, many questions were generated and addressed during IWG workshops. One area of critical interest related to the potential time/space scale mismatch or match among features of the ecosystem. From a physics perspective, the eastern shelf has distinct regions or strata that are dominated by different physical processes. This is strongly evident in an across-shelf direction going from the more oceanic-like outer shelf waters to the strongly two-layered middle shelf and then shoreward into a water column that often is without vertical structure. (Stabeno *et al.*, 1999a) show that differences in advection occur within the previously defined latitudinal strata (southeastern, central and northern shelf; Schumacher and Stabeno, 1998). For this reason, some of the physical observations were partitioned into areas within the NMFS strata (Section 3.3.4). Some data sets, however, would become too noisy if the spatial domain is reduced beyond some limit. For example, the estimates of pollock abundance from the bottom trawl survey (Fig. 3.4) can be grouped in the same areas used for the ice index. However, it was the consensus of the IWG that this time series contains too much variation and that the integrated values (i.e., the commonly used time series of adult or age-1 pollock throughout the eastern Bering Sea) provided the appropriate time series of abundance.

The IWG members also felt that it was important to consider the local/regional impact of larger-scale indices, seeking relationships between physics and biology. For example, when using a hemispherical index (e.g., Arctic Oscillation, PDO, NPI), one should first consider how it is manifested on the regional or local scale. This also applies on finer spatial scales, e.g., how representative are winds measured at St. Paul Island to mixing processes in inner Bristol Bay? While zero-order approaches have some value, their results can be misleading. For example, several studies use the OSCURS model to transport planktonic stages of various species. In these simulations, only one release site is used to initialize trajectories. As results from the NEPROMS model have shown (Section 3.3.7), changes in initial location can result in significantly different trajectories.

3.3 Development of Environmental Indices

3.3.1 *Indices of stratification, potential supply of nutrients to the upper mixed layer, and turbulence experienced by larval pollock (Carol Ladd and Phyllis Stabeno)*

We used the Price-Weller-Pinkel (Price *et al.*, 1986) one-dimensional, mixed layer model to simulate the establishment of stratification and subsequent mixing over the southeast Bering Sea shelf during summer. We selected the location (56.9°N, 164.1°W) to coincide with the site of FOCI biophysical mooring 2. Observations collected at this mooring provide 7 years of data that were used to validate model results. The possible mechanisms that could relate mixed layer depth to differential survival of young-of-the-year pollock include: (1) food limitation due to lack of renewal of nutrients from deeper waters or mixing of food particles through a larger volume of water, and (2) changes in the upper layer thermal field that impact physiological processes (timing of prey production and duration of the development of larvae to the first feeding stage) and community composition (appearance of new predators).

The model calculates the density and wind-driven velocity profile in response to imposed atmospheric forcing (discussed below using the method of Price *et al.*, 1986). Model simulations were initialized with a vertical temperature profile derived from the NCEP Reanalysis (Kalnay *et al.*, 1996). We used the sea surface temperature (SST) from May 1 combined with a weak thermocline ($\Delta T = 0.5^\circ\text{C}$) between 10 and 20 m. The model is then forced with winds and heat fluxes from the reanalysis and run from 1 May through 30 September 30 of each year. Comparisons with data show that the model reproduces mixed layer depth, timing of stratification set-up, and mixing events quite well.

The following assumptions and caveats should be noted:

- The model is one-dimensional. Hence, advection is assumed unimportant. Advection over the middle shelf is generally weak (Schumacher and Kinder, 1983; Schumacher and Stabeno, 1998). At times, however, currents have resulted in transport of salt and nutrients at this location (Stabeno *et al.*, 2001). In general, the assumption of no advection is likely good at this site, but it would have to be evaluated for other locations.
- The model is initialized with 1 May SST from the NCEP reanalysis. This time series has errors on the order of $\pm 0.5^\circ\text{C}$ when compared to in situ observations collected at site 2 between 1996–2001. These errors are well within the magnitude of interannual variability in the NCEP SST (the standard deviation over 40 years is $\sim 1^\circ\text{C}$). Summer heat content and SST of the model results, however, are dependent on the initial temperature profile and will reflect errors in that profile.
- Based on comparisons between model simulations and observations at site 2, salinity appears to have only a minor impact on stratification and mixing processes. Waters of the middle shelf domain exhibit weak

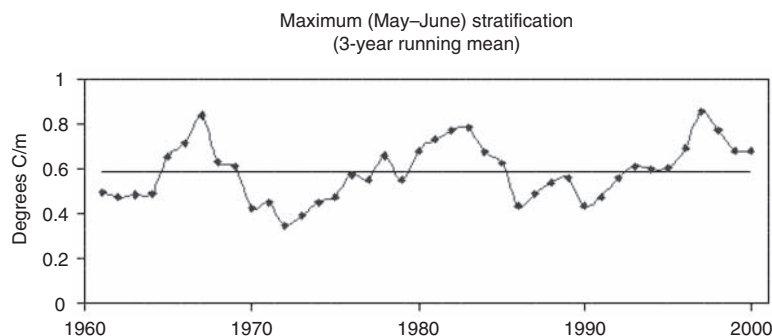


Figure 3.5: Maximum over May/June of vertical stratification maximum.

horizontal and vertical gradients in salinity (Coachman, 1986), and the time series of salinity measurements are sparse. Therefore, salinity is kept constant (31.65 psu) throughout the model runs.

- The model includes a diffusive term that results in a slightly weaker thermocline than observed. Without diffusion, the thermocline becomes too strong, resulting in SSTs that are too warm.
- Although the model simulates mixing processes in the upper layer quite well, the bottom mixed layer is not reproduced. Over the middle shelf, the water column exhibits a strongly stratified two-layer structure (in temperature) with a wind-mixed surface layer and a tidally mixed bottom layer (Schumacher and Stabeno, 1998). The model does not include any tidal mixing.

Results. Table 3.1 contains the stratification indices developed from this research. Interannual variability in mixing conditions can be evaluated using the model hindcasts. Model results show that the stratification maximum during May/June of each summer has varied on an approximately decadal time scale (Fig. 3.5) with maxima in 1967, the early 1980s, and 1997, and minima in the early 1970s and late 1980s. We note that this signal is not in phase with the accepted regime shifts (1976–1977, 1989, and perhaps 1998) observed in physical and biological time series for the eastern Bering Sea (Hare and Mantua, 2000).

When stratification is established in the spring, it provides an index of the timing of the spring bloom (Fig. 3.6) based on classical critical depth theory (Sverdrup, 1953). Interannual variability in the date of stratification is high with little indication of variability on decadal time scales. The stratification date averages 18 May and ranges between 10 May and 25 June.

The number of mixing events over the summer (Fig. 3.7) provides an index of the potential (some nutrients must still exist in the lower layer) amount of nutrient entrained into the mixed layer and of conditions that relate to decreased survival of pollock larvae (Bailey and Macklin, 1994). A high number of mixing events in a given year may indicate higher primary production and increased mortality of pollock larvae.

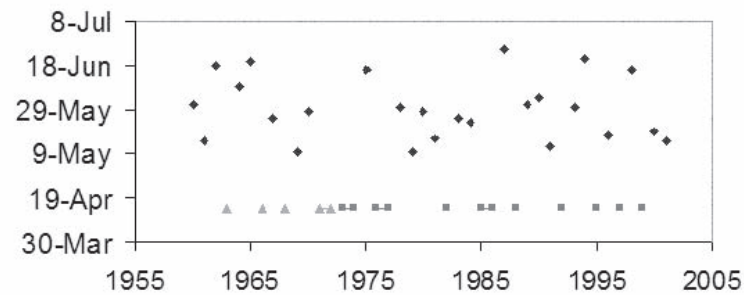


Figure 3.6: Date when maximum $\Delta T/\Delta z$ first is $>0.2^\circ\text{C}/\text{m}$ and occurs at a depth that is <25 m, for more than 1 day. Squares (ice data based on satellite images) and triangles (ice data based on shipboard observations) represent years when there was ice after 1 April, and an ice-associated bloom would have been expected (Stabeno *et al.*, 2001).

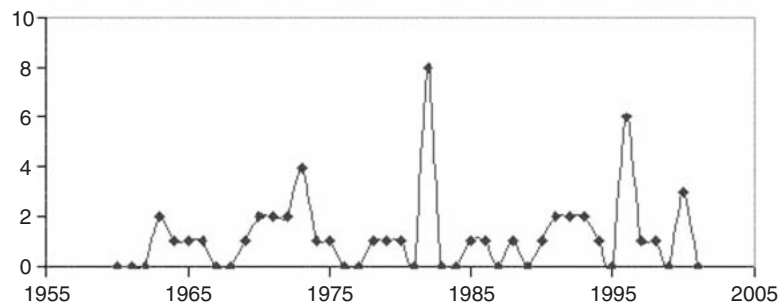


Figure 3.7: Number of times between the stratification setup date and 31 August when 3-day smoothed MLD increases >5 m in a day.

Temperature is important to the development of pollock eggs with eggs being slower to hatch in colder conditions (Blood, 2002). Temperature also affects the production of zooplankton (Coyle and Pinchuk, 2002b). The water column temperature on the stratification date (Fig. 3.8) may influence the coupling between the spring phytoplankton bloom and zooplankton prey for first feeding and older pollock larvae. Water column temperature on the stratification date varies between less than 1°C in 1991 to over 4°C in 1987 with high interannual variability, especially after 1980.

Future work. In order to expand on the present results, the model is being modified to track entrainment of water into the mixed layer. This will enable quantitative estimates of nutrient flux into the mixed layer over the summer. Another option would be to include a nutrient-like tracer, kept constant in the bottom layer and depleted over some time scale in the mixed layer.

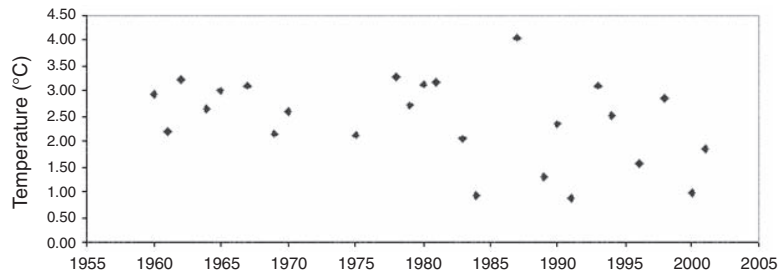


Figure 3.8: Water column average temperature on the stratification date. No temperature is shown for years when ice was present after 1 April.

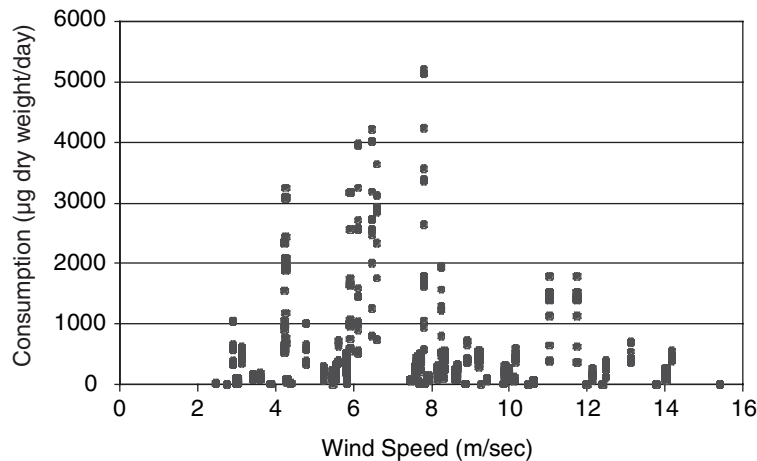


Figure 3.9: IBM output showing consumption as a function of wind speed.

3.3.2 An index related to wind turbulence and feeding success (Bern Megrey and Nick Bond)

Using a process-oriented, individual-based model (IBM) of pollock fish larvae, which incorporated a detailed description of the turbulence/contact rate/feeding success process (Megrey and Hinckley, 2001), we evaluated the relationship between the model-predicted influences of wind-generated turbulence and feeding. Output from the model (Figs. 3.9 and 3.10) conforms nicely to the theory (MacKenzie *et al.*, 1994) by the indication of a well-defined peak in consumption at intermediate wind speeds. Because of the high variability in the model data, we estimated the wind speed that generated optimum consumption (Fig. 3.11) by fitting a quadratic line through wind speed and consumption data, averaged by Julian day over the period DOY 102-164, the period when pollock are in their early larval stage. The wind speed that generated maximum consumption was derived by taking the derivative of the fit quadratic equation and setting it to zero. Optimum feeding (540 μg dry weight per day per individual) was at a wind speed of 7.1 m s^{-1} .

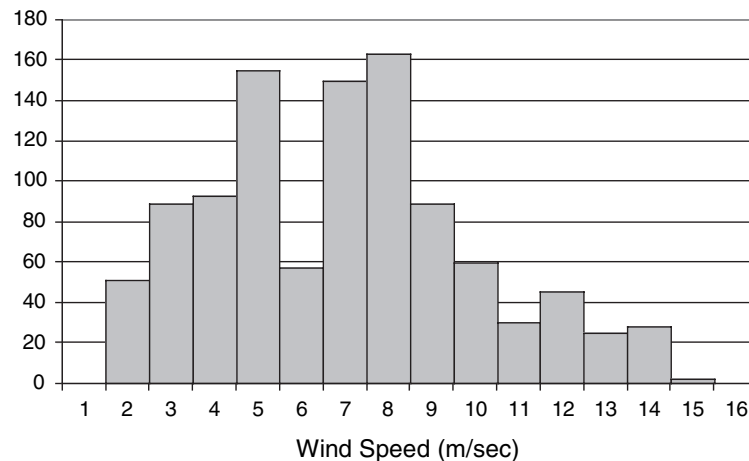


Figure 3.10: Frequency histogram of wind speeds used to force the IBM model.

Using Fig. 3.11, we arbitrarily defined the range of optimum feeding to be $\pm 15\%$ of the optimum level ($486 \mu\text{g}$ dry weight per day per individual). The wind speeds corresponding to a feeding level of $486 \mu\text{g}$ were 4.8 and 9.5 m s^{-1} . These points are indicated in Fig. 3.11 by the two circles on either side of the optimum circle. Thus, the range of wind speeds that provide “favorable feeding” would be 4.8 to 9.5 m s^{-1} . At wind speeds $>9.5 \text{ m s}^{-1}$, increased turbulence negatively affects feeding, and at wind speeds $<4.8 \text{ m s}^{-1}$, feeding is less than optimal because wind speeds are not sufficient to enhance the prey contact rate. Table 3.1 presents the indices developed for wind mixing.

There are some caveats that must be considered concerning this research. First, results are from a model experiment, not a laboratory experiment. Simulations were carried out on Shelikof Strait walleye pollock. However, results should be applicable to Bering Sea pollock as the feeding/contact-rate/turbulence processes should still be valid. Wind induced turbulence was not the only major process in the IBM model. The IBM was very detailed and included many other biological processes that would have affected the outcome of the simulations.

3.3.3 Variations in net short wave radiation: Toward development of an index of when sufficient light exists for primary production (Jeff Napp and Nancy Kachel)

The timing of the spring phytoplankton bloom is quite variable in the southeastern Bering Sea. It can occur anytime from the late winter to late spring, but it appears potentially to be predictable from prevailing environmental conditions (i.e., presence or absence of sea ice, frequency of storms, and erosion of the water column stability; Sambrotto *et al.*, 1986; Niebauer *et al.*, 1995; Stabeno *et al.*, 1998; Eslinger and Iverson, 2001; Hunt *et al.*, 2002a). Thus, it is conceivable to model the initiation of the spring phytoplankton bloom, which has significance to ecosystem dynamics. The dominant path-

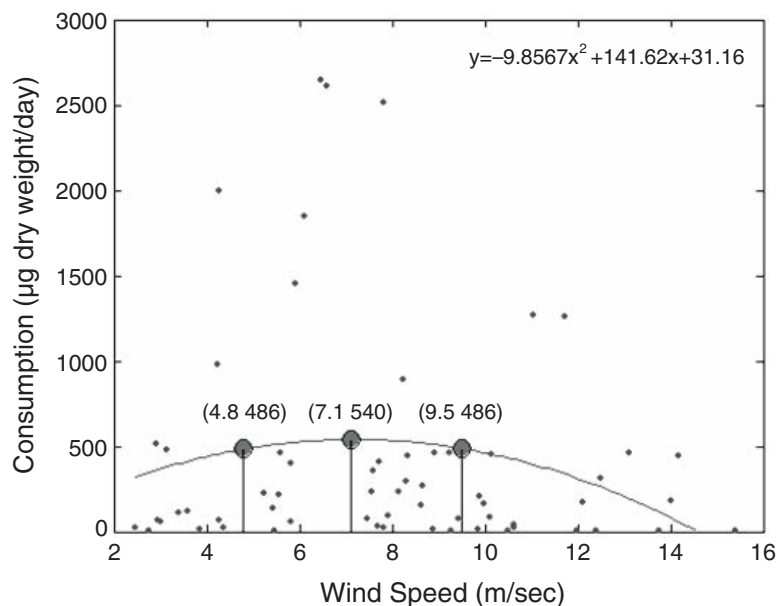


Figure 3.11: Estimates of the wind speeds required to generate optimum feeding.

ways of carbon cycling (pelagic versus benthic) as well as the temporal match or mismatch of larval pollock and their prey are dependent on the timing of the spring phytoplankton bloom (Napp *et al.*, 2000; Hunt *et al.*, 2002a). A strong case has been made that the timing of the bloom is dependent on the current atmospheric regime, and that it plays a key role in determining whether the ecosystem is controlled by bottom-up or top-down processes. Thus, prediction of the timing of the spring bloom would assist ecosystem managers in their assessment of the status and trends of the Bering Sea ecosystem (Hunt *et al.*, 2002a). The goal of the present exercise was to predict the earliest date that available light is sufficient to support a bloom and to begin an examination of interannual variation in this date.

Daily average net short wave radiation (NSWR) was extracted from the National Center for Atmospheric Research/National Center for Environmental Prediction (NCAR/NCEP) Reanalysis data set. We examined average NSWR for the period April 1–June 30 during 1972–2001 for three sites: inner Bristol Bay (IBB) at 58°N, 159°W, middle shelf domain (MSD) at 57.5°N, 165°W, and northwest central shelf domain (NWCSD) at 60°N, 170°W. The effect of latitude is evident, with the northernmost station receiving about 19% less energy (W m^{-2}) from 1981 onward (Fig. 3.12, Table 3.1). The MSD and IBB time series appear coherent, and are in phase with the NWCSD station from 1972–1983 and 1995–2001. During the intervening period, the time series appear to be out of phase by $\sim 180^\circ$. Correlation between the MSD and other two stations is significant and positive, although the amount of variance explained between the MSD and IBB is higher ($R^2 = 0.58$) than the MSD and NWCSD ($R^2 = 0.43$).

From our analysis, several conclusions can be drawn. First, if monitoring

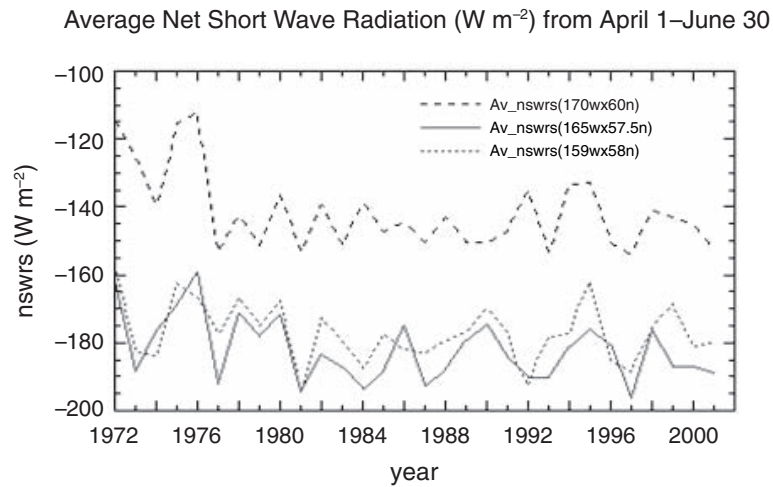


Figure 3.12: Average net short wave radiation from 1 April–30 June (W m^{-2}).

of a smaller set of stations is desired, then it is recommended that there is at least one station in both the southeast and northwest portions of the eastern Bering Sea shelf. This is due to both latitudinal and local meteorological conditions, which appear to drive the southeast and northwest systems in or out of phase. The second feature seen in the data is the large degree of interannual variability. The data show frequent positive and negative deviations from the long-term daily mean. Of these two fluctuations, the negative deviations qualitatively appear to be more frequent and pronounced than the positive ones. The sustained positive deviations will tend to promote an earlier bloom (ignoring wind mixing), and prolonged negative deviations will tend to delay the bloom. See Section 3.6 for suggested further research.

3.3.4 Indices related to sea ice (Sigrid Salo and Phyllis Stabeno)

Sea ice is a prominent feature of the eastern Bering Sea shelf, and several mechanisms exist that connect sea ice to biological processes. The phytoplankton bloom associated with the presence of sea ice (Stabeno *et al.*, 1998) influences the timing of zooplankton prey availability for first feeding pollock larvae. The size and magnitude of the following summer's cold pool depend on sea ice cover (timing and persistence) and can influence adult fish distribution and intensity of cannibalism.

Several indices exist for assessing the annual influence of sea ice on the continental shelf of the eastern Bering Sea. Niebauer (1998) and Niebauer *et al.* (1999) used the percentage of ice cover over the entire shelf. Another index, used to relate physical characteristics to changes in fish populations, was based on the presence of ice along the longitude of 169°W (Wyllie-Echeverria and Wooster, 1998). Both have shortcomings. The percent ice cover provides no information regarding changes in the spatial patterns of the sea ice, and the longitudinal index is not always spatially representative.

To examine sea ice characteristics on a finer spatial scale, we calculated

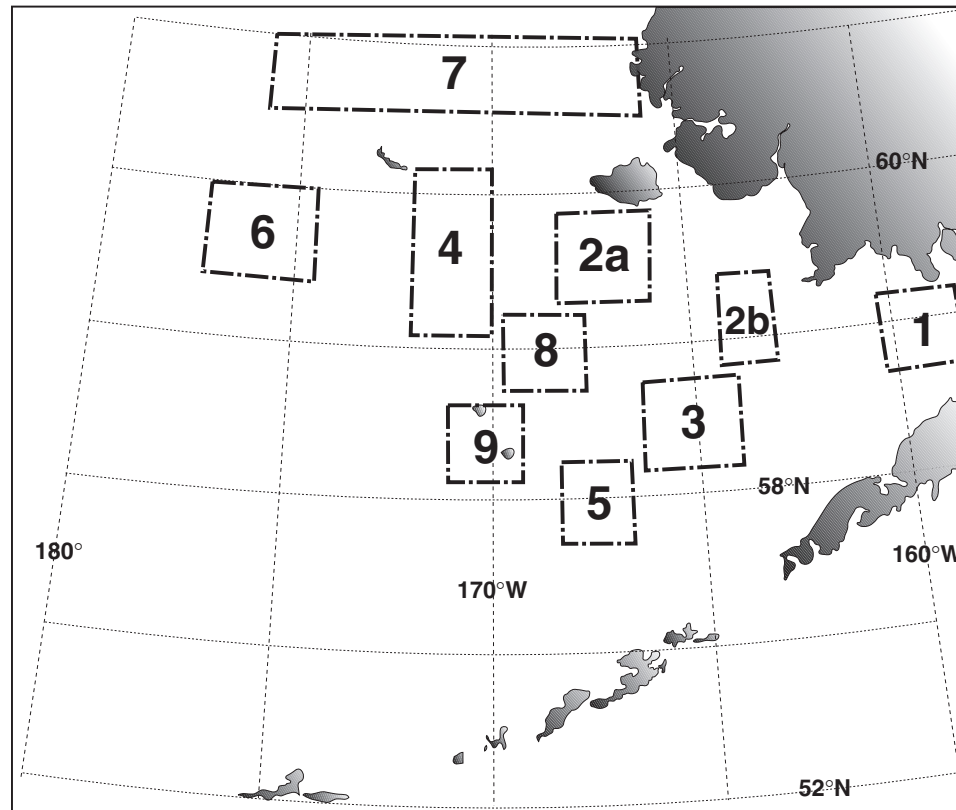


Figure 3.13: Strata used to calculate ice concentration.

ice concentration in the ten strata shown in Fig. 3.13. The ice concentration data are on a 0.25° grid and were obtained from two sources. Data from 1972 to 1994 came from the compact disk of Arctic and Antarctic ice concentrations produced by the National Ice Center, Fleet Numerical Meteorology and Oceanography Detachment (FNOC), and the National Climatic Data Center. To extend the time series to 2001, we digitized charts from the Anchorage Weather Service Forecast Office. The National Ice Center offers one chart of ice concentrations per week, and we continued to use that interval.

Using the results from area 9 (which includes longitude 169°W that was used in a previous index) and area 3, strong differences are evident as shown in Figs. 3.14 and 3.15. This comparison clearly shows some common features, i.e., the years of greatest ice extent occurred prior to the 1976–1977 regime shift. For the most part, however, the sea ice concentration is much less in Area 9 than in Area 3. Analyses of spatial patterns in sea ice cover have revealed both earlier transition to spring over the middle and outer shelf. The ice concentration results for all strata are presented in some detail below in order to highlight the rich nature of the original time series and the inherent spatial variability that exists over the shelf:

Area 7: Ice remains for a long period, occurs earlier and retreat is latest

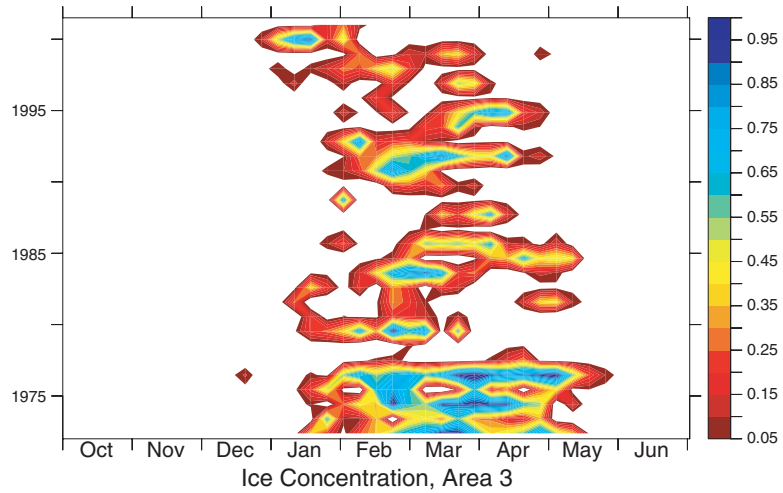


Figure 3.14: The time series of sea ice concentration in Area 3.

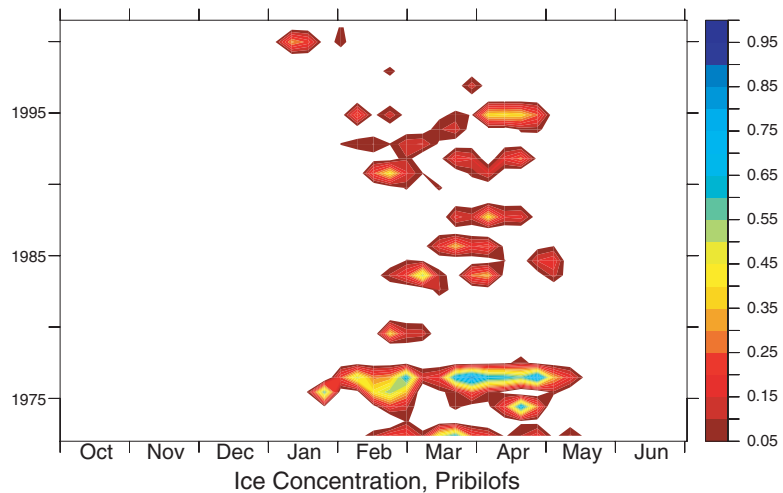


Figure 3.15: The time series showing ice concentration in Area 9.

of all the areas. The date of last ice is typically about 15 June, with the ice disappearing over a long period (about 1 month from full to no coverage). Most of the change among years occurs on the interannual time scale rather than decadal.

Area 2b: Some decadal period in the ice coverage, and disappearance occurs quicker than in Area 7.

Area 2a: very similar to 2b.

Area 4: Ice concentration shows the greatest variability here of all the areas. There is similarity in ice concentration with patterns in 2a. There appears to be little difference between these two areas in the length of time that the ice remains; the major difference is the later arrival of ice in Area 4.

The above are the four areas with the most extensive ice.

Area 6: The concentration of ice changes immensely each year. This area is dominated by interannual variation, and it has distinctly less ice than the other areas. In some years, there is little or no ice at all.

Area 8: (contains mooring site 4) The concentration of ice here shows large variability in percent of concentration. The time of maximum concentration varies throughout the years: one year it occurred in January, while in another year it occurred about May 1.

Area 3: (contains mooring site 2) We know most about what is occurring at this location from the long-term moored instruments. Interannual variability is the dominant mechanism in the spectrum of ice concentration here.

Area 1: This area is in a region where ice can form locally. The ice observations show that there is huge interannual variability in the concentration of ice, which provides a most surprising result.

Pribilof I.: Some of the variation in ice concentration here occurs because of the influence of the islands on regional and tidal currents. St. George Island typically has minimal ice compared to St. Paul Island. The patterns of ice concentration are very distinct from other areas. For example, in Area 7 there is ice 5–6 months of year, while there may be none at all around the Pribilof Islands.

Area 5: The warmer slope waters bathe this area, and ice is a transient feature. There were significant concentrations in the early 1970s (cold period), and, after the regime shift of 1976/77, ice was an infrequent visitor to this area. The dominant energy of this area occurs in the year-to-year variability.

For indices of sea ice (Table 3.1), the average percent concentration of sea ice within a rectangular region bounded by 58°N, 170°W and 57°N, 165°W was computed during the period 15 March to 15 April over the active research years of SEBSCC.

Sea ice has a marked impact on the ecosystem of the eastern Bering Sea. It provides habitat for marine mammals, and its presence is related to timing and magnitude of primary production (e.g., Stabeno *et al.*, 1998; Hunt *et al.*, 2002a). While a single index of ice can provide an indication of ecosystem characteristics, this analysis demonstrates that a single index of ice concentration is not valid for the entire SEBSCC study area. Because time series observations exist, indices can be created for any region of interest over the shelf.

3.3.5 Indices related to the cold pool and adjacent fronts (Peggy Sullivan)

Cooling and mixing associated with sea ice advance help to condition the entire water column over the Middle Shelf Domain, generating the cold lower layer of water known as the “cold pool” (Schumacher and Stabeno, 1998; Stabeno *et al.*, 1998). With seasonal heating, the lower layer becomes insulated and temperatures often remain below 2.0°C. The area of this cold pool varies by $\sim 2.0 \times 10^5$ km² between maximum and minimum extent. The

mechanisms that connect the cold pool to biota include changing habitat location (species composition) and alteration of biological rates.

Temperature cross sections along two southeastern Bering Sea transects are assessed over the years, 1996, and 1998–2000. MicroBathythermograph (MBT) temperature profile data from the Alaska Fisheries Science Center (AFSC) annual trawl surveys were used. Fig. 3.16 shows the areal extent and well-gridded structure of the trawl survey data, with data-collection sites shown by blue triangles, and red triangles marking the two transects which were processed and used for present purposes. The transects were chosen to represent distinctive regions near the perimeters of the trawl area, while still residing within solid data-coverage range for the entire area. Transect 1 (T1), the more northwesterly line, optimally contains nine data-collection points, while Transect 2 (T2), the more southeasterly line, optimally contains 11 data-collection points. Not all points exist for each year. Kachel *et al.* (2002) provide insight into processes related to the cold pool and inner front based on temperature, salinity, and dissolved nutrient observations, and Stabeno *et al.* (2002) provide insight into processes along the 70-m isobath.

Observing successive years across the same transects allows a comparative view of the behavior of the middle shelf cold pool, its year-to-year variations and overall shelf temperatures. The cold pool is well defined for all years along T1 (Figs. 3.17–3.20). This transect is not close to shore, so the coastal shelf is not well represented. The warm years of 1996, 1998, and 2000 had relatively warmer surface waters. During 1999, overall temperatures are colder, and the cold pool is cooler and shifted more shoreward. For both 1999 and 2000, the cold pool is shallower than in 1996 and 1998.

At transect 2, Fig. 3.21 shows a well-defined cold pool in 1996, deeper than in subsequent years, with horizontal temperature variability and moderately warm temperatures. During 1998–2000 (Figs. 3.22–3.24), the cold pool is more horizontally dispersed. The year 1998 had warmer overall temperatures, and the colder years 1999 and 2000 showed cold water more shoreward into the vertically mixed coastal shelf. The cold pool index in Table 3.1 shows the estimated area (km²) of water colder than 2°C in the vertical section of the T1 transect.

It should be noted that MBT trawl survey data from the AFSC are the subject of a data rescue, and, when completed, will be a rich data resource. Data profiles from 1992 through 2000 number approximately 3000. The physical data portion of the survey is being processed with normal PMEL methodologies, quality control, and web placement.

3.3.6 Pribilof age-0 pollock as an index of pollock year-class strength (Jim Ianelli)

Each year the EBS pollock stock is analyzed for fishery management purposes. This analysis consists of an integrated statistical assessment based on several different types of observations. The primary data analyzed include annual bottom-trawl surveys of the entire shelf area (within the U.S. EEZ), bi-annual echo-integration trawl (EIT) surveys of this region, annual fishery catch data from scientific observers aboard fishing vessels, and estimates of

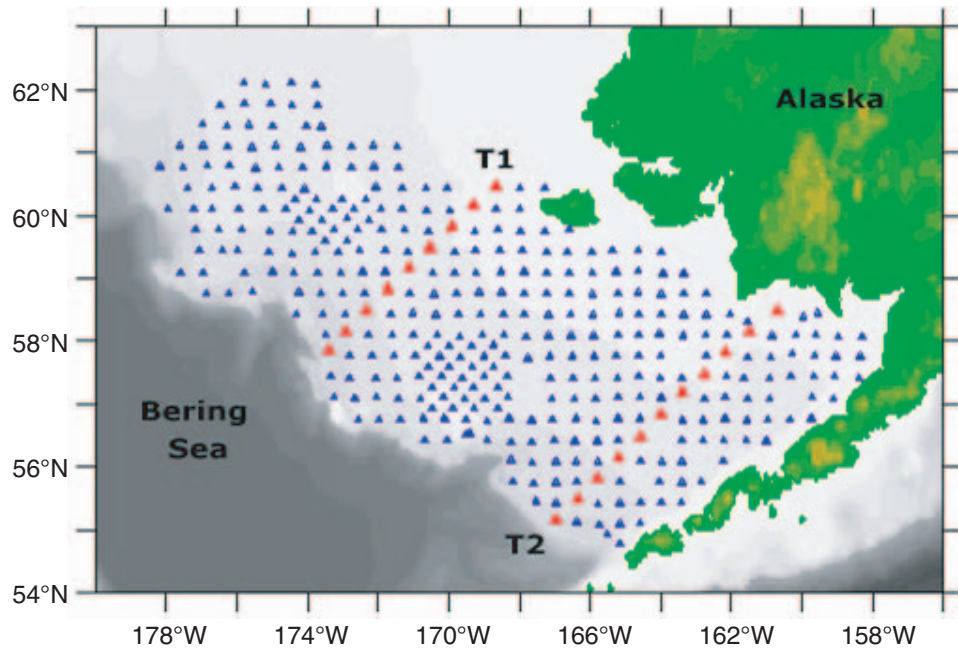


Figure 3.16: Trawl survey data collection grid in the Bering Sea. Data locations from the 1996 data set were used. Red triangles indicate transects 1 and 2.

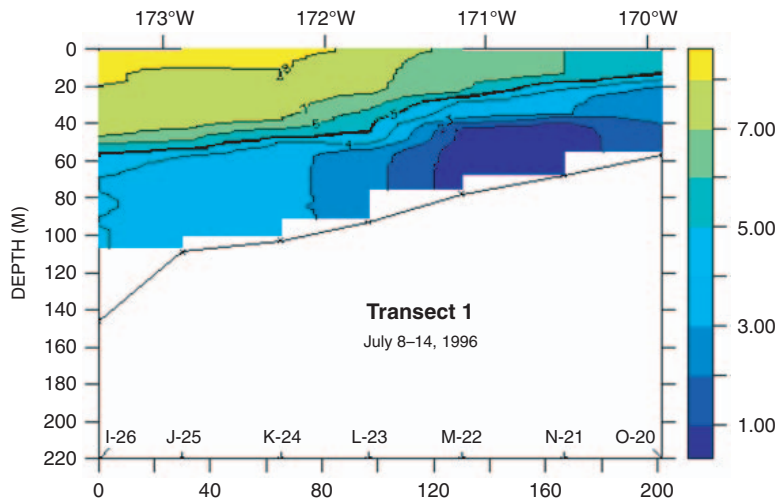


Figure 3.17: Temperature contours along T1 for 1996.

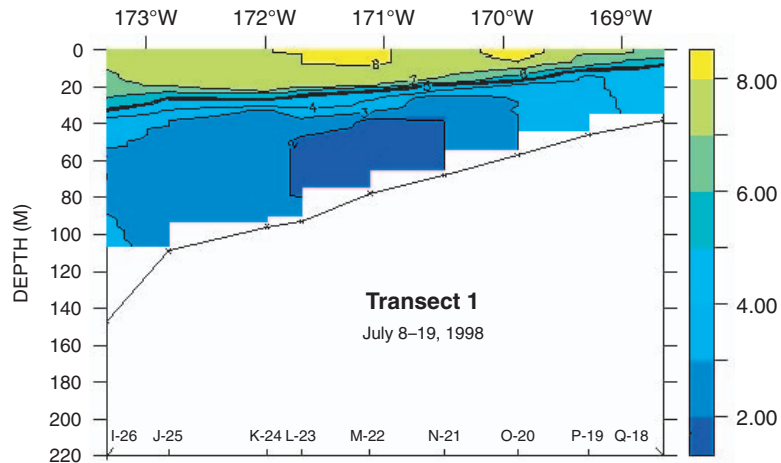


Figure 3.18: Temperature contours along T1 for 1998.

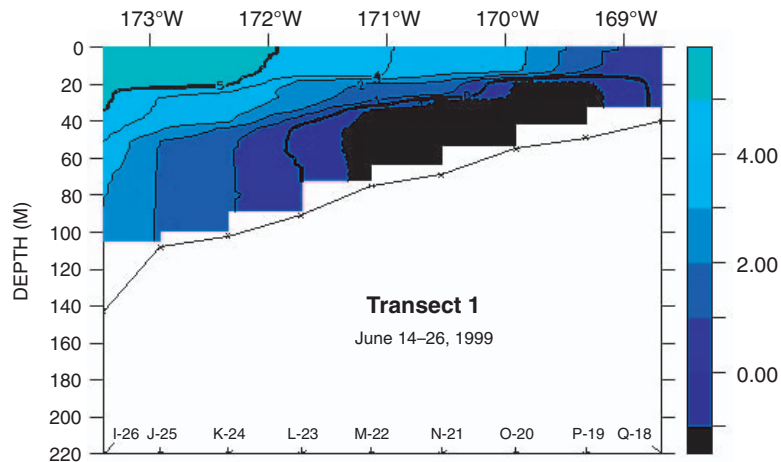


Figure 3.19: Temperature contours along T1 for 1999.

biological characteristics (e.g., age composition, growth, and maturation). These assessment analyses lead to recommendations on risk-averse harvest levels for the coming year.

The risk-averse aspects of harvest recommendations include levels of uncertainty in both the observations and the physical processes affecting the population. For example, pollock in this region are well known to have highly variable year classes (coefficients of variation on the order of 60%). As this variability propagates through the population, a key variable in quota determination is affected: estimated pollock biomass. It is therefore useful to be able to estimate reliably the abundance of incoming (pre-recruit) pollock.

One suggestion is that for a relatively small sampling effort, abundance of age-0 pollock around the Pribilof Islands can provide a useful index of year-class strength. Preliminary comparisons (Swartzman *et al.*, 2002) of such an

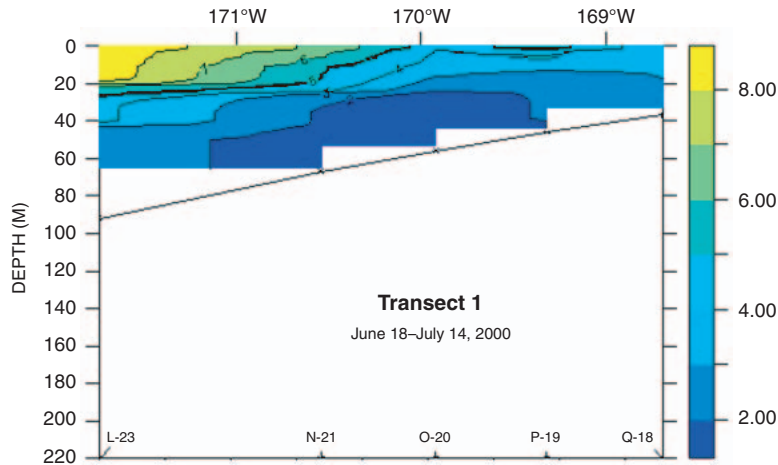


Figure 3.20: Temperature contours along T1 for 2000.

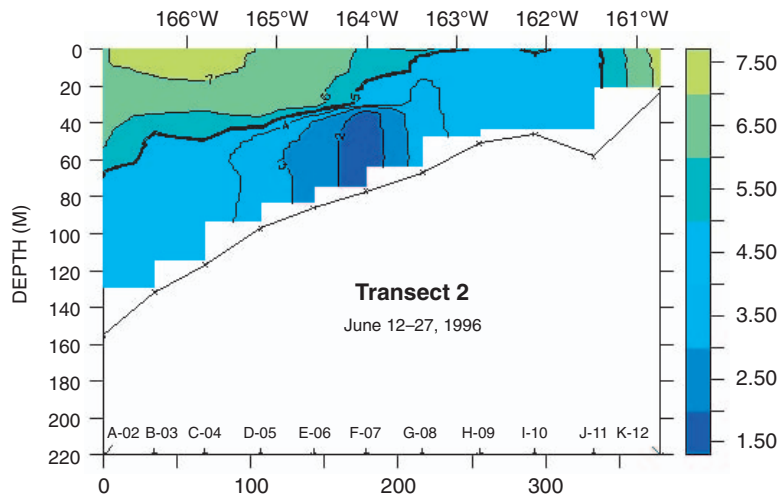


Figure 3.21: Temperature contours along T2 for 1996.

index with results from assessment analysis (based on age compositions from the fishery and two independent surveys, abundance indices from two surveys, growth rates, maturity information, natural mortality rates, and catch of the fishery; Ianelli *et al.*, 2001) suggest that an index of this type might prove useful (Fig. 3.25, Table 3.1). This is particularly appealing when one examines similarly constructed indices with other pollock surveys since both the bottom trawl and EIT surveys provide some indication of pre-recruit abundance at later stages (Figs. 3.26 and 3.27). The root mean squared errors for these three indices (relative to the assessment model prediction in log-space) are:

Note that in the assessment analyses, the overall abundance estimates (e.g., the area-swept estimate of total population numbers) are treated in-

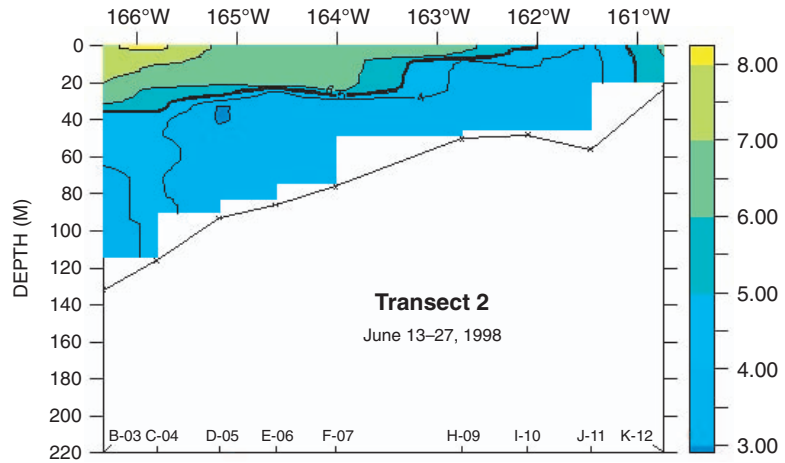


Figure 3.22: Temperature contours along T2 for 1998.

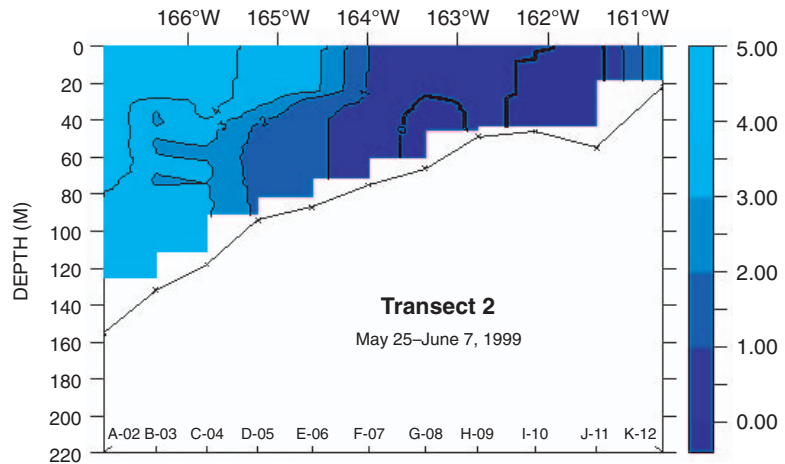


Figure 3.23: Temperature contours along T2 for 1999.

Pribilof Age 0	Age 1 Bottom trawl survey	Age 3 EIT survey
0.725	0.532	0.713

dependently from estimates of the age composition. This appeals to the way the population is sampled and sub-sampled for age compositions and avoids independence problems of statistically fitting several separate sets of indices-at-age. Furthermore, the indices as presented above are only for representation and do not reflect the fact that the assessment model allows for changes in age-specific availability over time (Ianelli *et al.*, 2001).

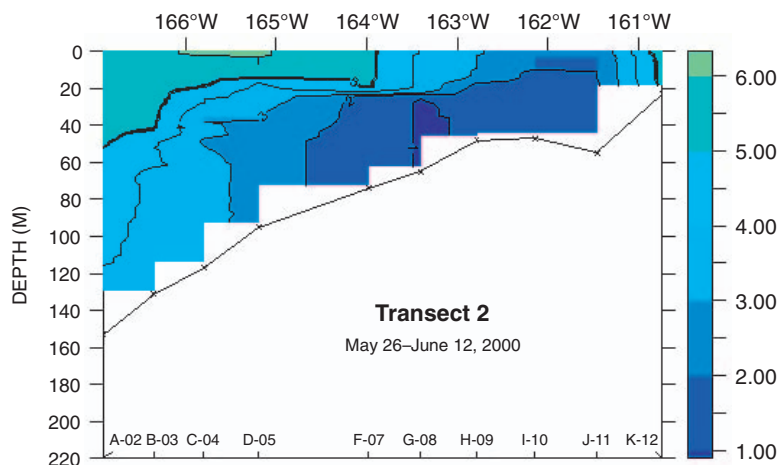


Figure 3.24: Temperature contours along T2 for 2000.



Figure 3.25: Pribilof young-of-the-year index relative to assessment results from Ianelli *et al.* (2001). Units are arbitrary.

3.3.7 Model simulations

What is NEPROMS? (Al Hermann). The Regional Ocean Modeling System (ROMS) is a versatile, state-of-the-art, free-surface, hydrostatic, primitive equation, ocean circulation model developed at Rutgers University and UCLA. Details can be found in Haidvogel *et al.* (2000), Shchepetkin and McWilliams (1998), and Marchesiello *et al.* (2001), and on the ROMS web site (<http://marine.rutgers.edu/po/index.php>). The ROMS user community now numbers more than 200 scientists worldwide. The version of ROMS used for our simulations achieves distributed memory parallelism using the Scalable Modeling System developed at NOAA's Forecast Systems Laboratory.

Using this parallel version of ROMS, we have been implementing a suite of basin-, regional-, and local-scale circulation models, linked via one- (and

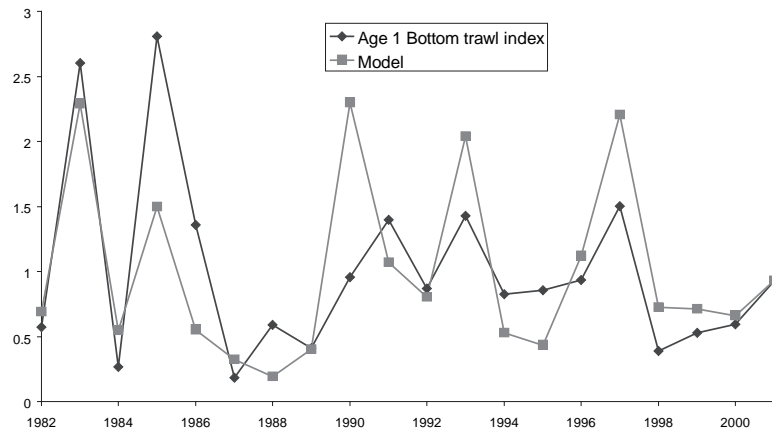


Figure 3.26: NMFS bottom trawl survey age-1 index relative to assessment results from Ianelli *et al.* (2001). Units in numbers rescaled to have a mean value of 1.

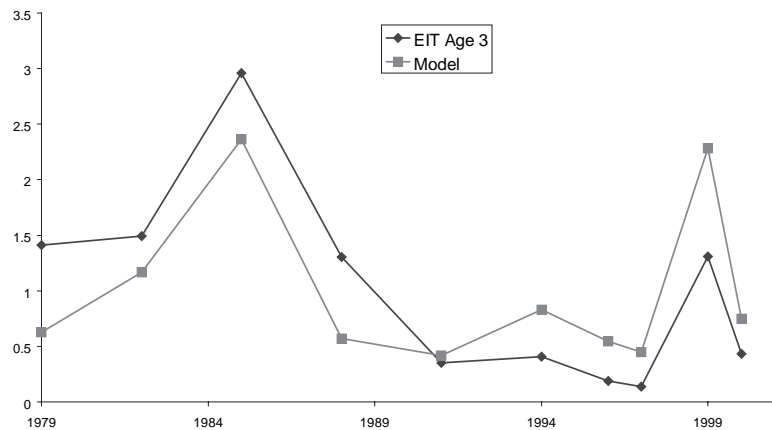


Figure 3.27: NMFS EIT survey age-3 index relative to assessment results from Ianelli *et al.* (2001). Units in numbers re-scaled. Note that the observations do not occur in every year.

eventually two-) way coupling. Figure 3.28 shows the set of nested modeling domains in current use, including: a basin-scale model encompassing the North Pacific Basin at 20–40 km resolution (NPac), a regional model at ~10-km resolution spanning the Northeast Pacific (NEP), and finally local models at ~3-km resolution in regions of specific interest [California Current System (CCS) and the Coastal Gulf of Alaska (CGOA)]. The NEP grid spans the area from Baja California up through the Bering Sea at approximately 10-km resolution, and was used for the simulations of the Bering Sea reported here. Additional information on these models (with snapshots and animations of model output) is available at <http://www.pmel.noaa.gov/~dobbins/nep.html>.

The NEP model is forced with daily average wind (converted to wind stress) and heat fluxes (sensible, latent, longwave, and shortwave) from the

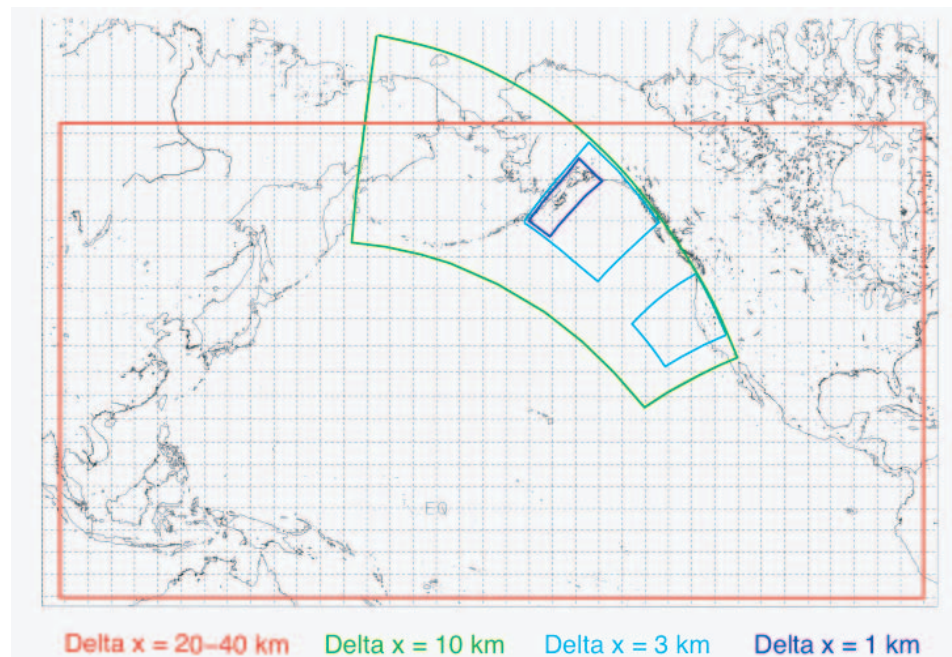


Figure 3.28: Nested modeling domains in current use for Pacific modeling, including: a basin-scale model encompassing the North Pacific Basin at 20–40 km resolution (NPac, red), a regional model at ~ 10 km resolution spanning the Northeast Pacific (NEP, green), and finally local models at ~ 3 km resolution in regions of the California Current System (CCS, light blue) and the coastal Gulf of Alaska (CGOA, light blue).

NCEP reanalysis project. No tidal forcing is included in these simulations. Model runs were initialized with Levitus monthly climatology for T and S fields. Hindcasts for a particular year were achieved by spinning up the NEP model from January of the previous year; for example, the model was spun up using daily NCEP values from January 1999–March 2000 for hindcasts of the period April–July 2000. Although even longer spin up would be preferable, 15 months is a sufficiently long period to evolve the appropriate mesoscale detail in the boundary currents and gyres (which is not contained in the coarse-scale Levitus-based initialization). It is also long enough to allow NCEP forcing to produce conditions (e.g., SST and currents) appropriate to the hindcast year (Fig. 3.29). Buoyancy input for the Gulf of Alaska was derived from the analyses of Royer (1982 and Old Dominion University, personal communication) and is added at the surface of the water column along the coast in the CGOA. The weakly dissipative algorithms for tracer advection in ROMS obviate the need for strong explicit mixing; here, explicit Laplacian horizontal mixing coefficients were set at $50 \text{ m}^2 \text{ s}^{-1}$ for momentum and $25 \text{ m}^2 \text{ s}^{-1}$ for temperature and salinity.

ROMS includes algorithms for passive float tracking in three dimensions. Floats can be seeded at arbitrary locations and times, and re-seeded as required for the numerical experiment. Output includes Lagrangian time

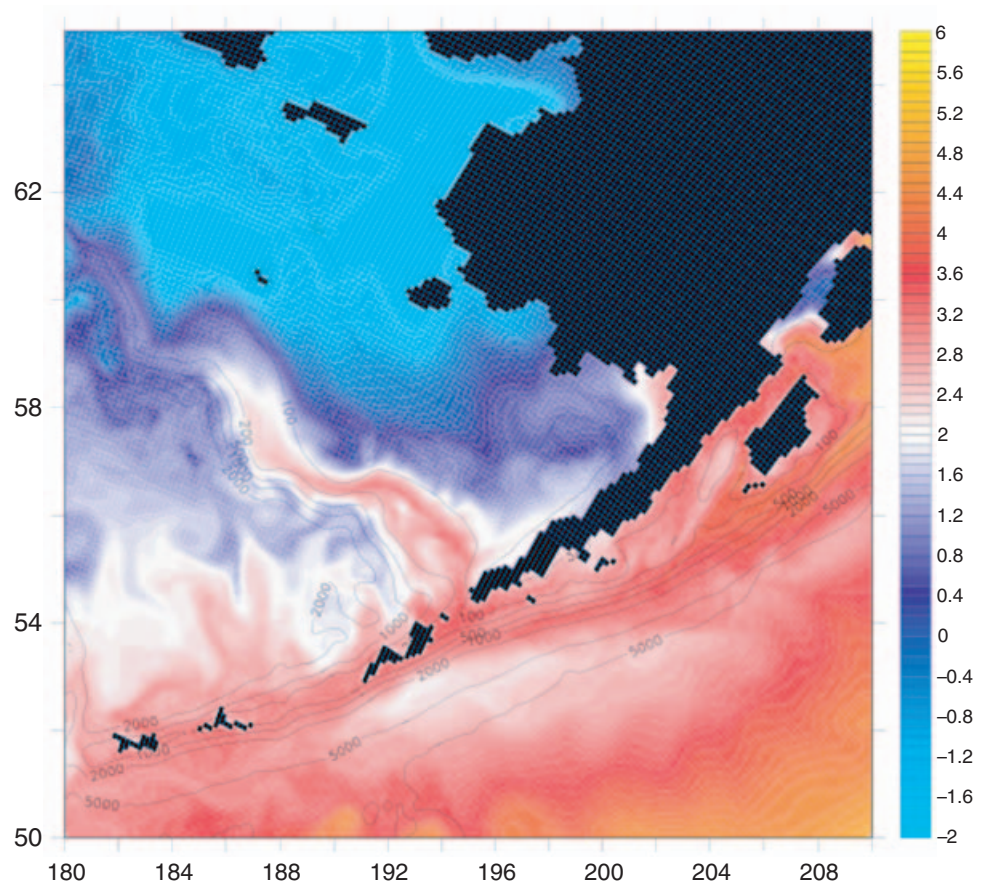


Figure 3.29: Model-generated sea surface temperature in the southeastern Bering Sea for 15 April 2000. Axes denote latitude ($^{\circ}$ N) and longitude ($^{\circ}$ E). Bathymetry is contoured in meters. Note the penetration of warmer waters from the Gulf of Alaska through Unimak Pass.

series of position, depth, salinity, temperature, and density. We have utilized this feature to track the temperature history of passive particles during NEP runs, as an approximation to the life history of passive planktonic organisms, e.g., pollock larvae.

ROMS simulations of pollock egg and larvae transport (Dylan Righi). Several mechanisms can connect transport of eggs and larvae to survival, including: transport to regions where predation is great due to cannibalism, and transport to regions where primary and secondary production is minimal (reduced prey availability). In this contribution, only the characteristics of the transport itself are addressed. The Northeastern Pacific Regional Ocean Model System (NEPROMS) was used to simulate drifter trajectories in the southeastern Bering Sea. Drifter tracking in ROMS is done using a fourth-order, predictor-corrector scheme. Drifters are allowed to move vertically. We currently have results for the years 1997–2001.

The simulated drifters are initialized over the eastern Bering Sea shelf just north of Unimak Island and to the northeast of Unimak Pass. This region

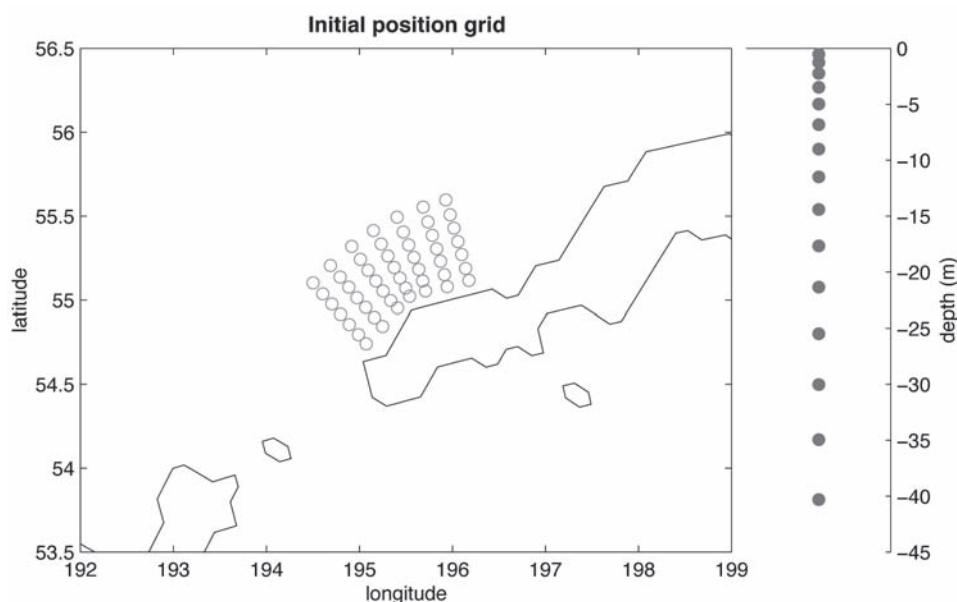


Figure 3.30: Simulated drifter initial horizontal (left) and vertical (right) positions.

is known to be an area of strong spawning for walleye pollock. The initial drifter positions fill out a 7×7 grid with horizontal separations of about 10 km (Fig. 3.30). Vertically, there are 15 drifters initialized at each grid point with maximum depths just over 40 m. The drifter initial positions are denser near the surface, replicating vertical egg distribution data collected in the Bering Sea (Kendall, 2001). Drifters are released on 1 April of each year and are tracked for 90 days.

Endpoints after 90 days for drifter trajectories from the 1997–2001 runs are shown in Fig. 3.31 (this plot shows all drifters at all depths). In all years, there is a strong tendency for trajectories to move to the northeast up the Alaskan Peninsula. The other common path is movement to the northwest along the 100-m isobath. These patterns are qualitatively similar to circulation schematics that were constructed from current, satellite-tracked drifter and hydrographic observations (e.g., Schumacher and Stabeno, 1998). The split between these two paths is seen clearly in the 1998, 1999, and 2001 drifter endpoints. In 1997, the full trajectory plots (not presented here) show that a subset of the drifters begin following the standard 100-m isobath path, but then currents change and drive them up the shelf to the northeast. The endpoints in 2000 are the result of strong turning to the northwest of trajectories that previously had been moving up the Alaskan peninsula. Further study of possible forcing mechanisms is needed to understand what leads to these years departing from the archetypal two-limbed flow.

The initial goal of this work was to compare simulated trajectories from a full primitive equation model with those from the Ocean Surface Current Simulations (OSCURS) numerical model. OSCURS computes daily surface current fields using daily sea level pressure and long-term mean geostrophic

current data. As such, it is a simpler model in terms of the physics involved and is much less computationally expensive. Wespestad *et al.* (2000) used OSCURS to create simulated trajectories in the Bering Sea. The initial grid used here was centered on the initial release point they used. Our trajectories for drifters released near the surface (0 to 5 m depth) show good agreement with the OSCURS results. However, our results show variation of trajectory endpoints with changes in both horizontal and vertical initial position. Figure 3.32 shows the full trajectories for the 2001 simulated drifters.

The upper left panel of Fig. 3.32 shows the tracks of all the drifters released for the run. The upper right and the bottom panels show drifter tracks as a function of their release depth. The first facet of these plots is that a drifter's endpoint depends largely on its initial horizontal placement.

The next point is that there is a strong dependence on release depth. The OSCURS 2001 trajectory moves a short distance to the northeast up the Alaskan Peninsula, as do the majority of the NEPROMS drifters released in the upper 5 m of the water column (upper right panel of Fig. 3.32). Nevertheless, with deeper release points comes a stronger divergence of the trajectory fates. In the 5–20 m and 20–40 m release bins, there are significant numbers of drifters that join the 100-m isobath flow to the northwest, with some even moving through Unimak Pass before turning back. OSCURS results completely miss this variation in particle fates.

As a working index of advection, Table 3.1 shows the fraction of each year's 735 simulated drifters that landed in the region bounded by 57°–58°N, 165°–170°W after 90 days.

3.3.8 A matrix for cataloging indices (Allen Macklin)

Early in the brainstorming process, members of the Indices Working Group suggested that a matrix would be a valuable data cataloging tool and an aid in developing and testing indices. At a minimum, a matrix would help with the housekeeping tasks of data tracking. At its fullest development, a matrix would be a multi-dimensional catalog of SEBSCC (and other relevant) data, accessible through the Internet, with direct links to referenced data collections. Presently, the character of the matrix is somewhere between the extremes. It is viewed as a dynamic document that is one of SEBSCC's legacies for future research in the region.

Figure 3.33 illustrates the Microsoft Excel version of the matrix. It is available by linking to "Phase III Working Groups" on the SEBSCC web site at <http://www.pmel.noaa.gov/sebscc>. Note that each index or data variable in column 1 (scrollable) is cataloged in two dimensions: time and space. Each index also contains a description, e.g., the yellow box in Fig. 3.33 describes the "Thermocline" index. Passing the computer's mouse over the cell containing the index name activates the description. To the right of column 1 are scrollable, color-coded columns for the years contributing to the matrix, 1972–2001. Each color-coded column is divided into four sub-columns: annual average, spring bloom, summer, fall overturn. These represent the important time scales and seasonal periods for the matrix. Cells

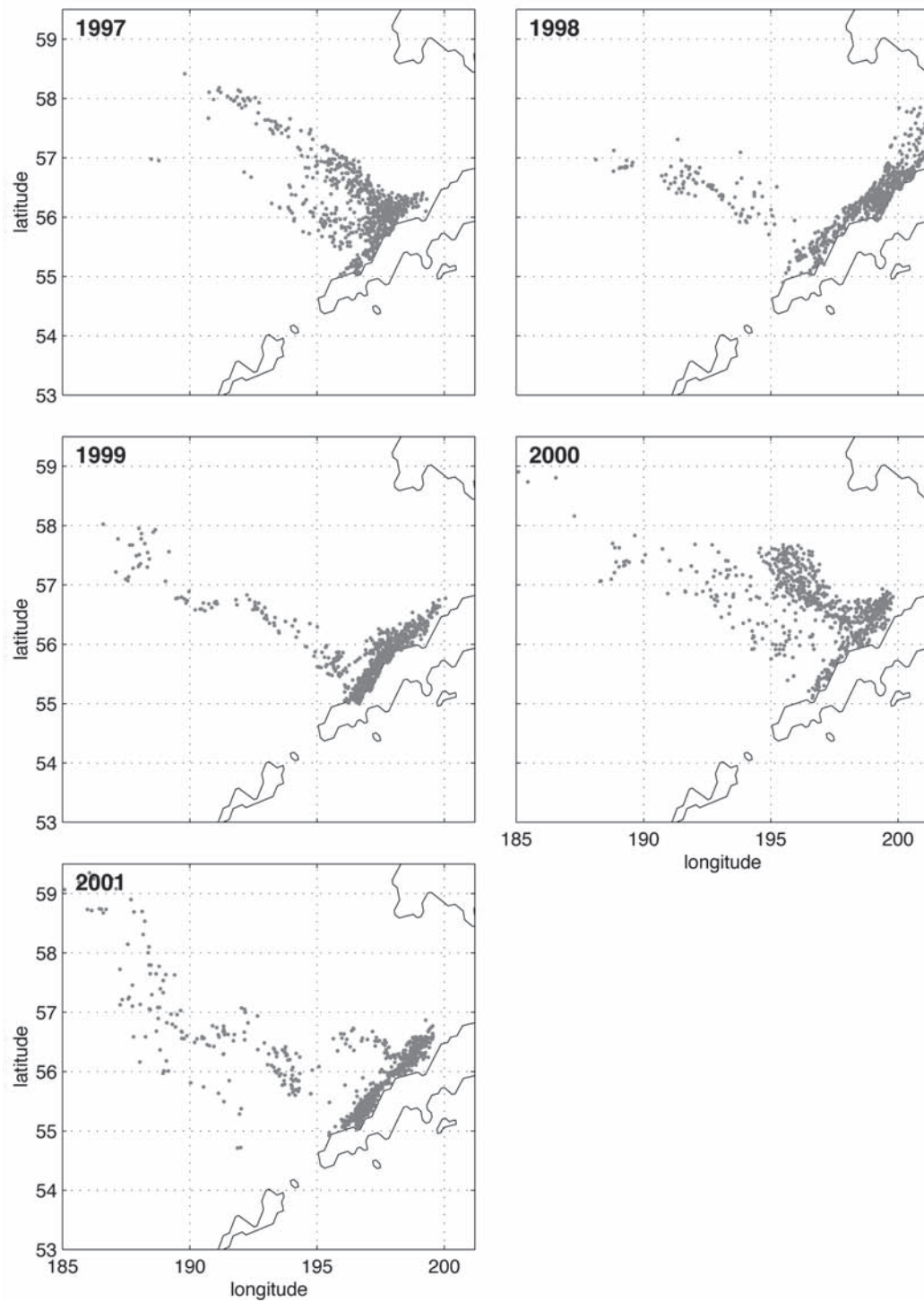


Figure 3.31: Endpoints for 90-day drifter trajectories for 1997–2001.

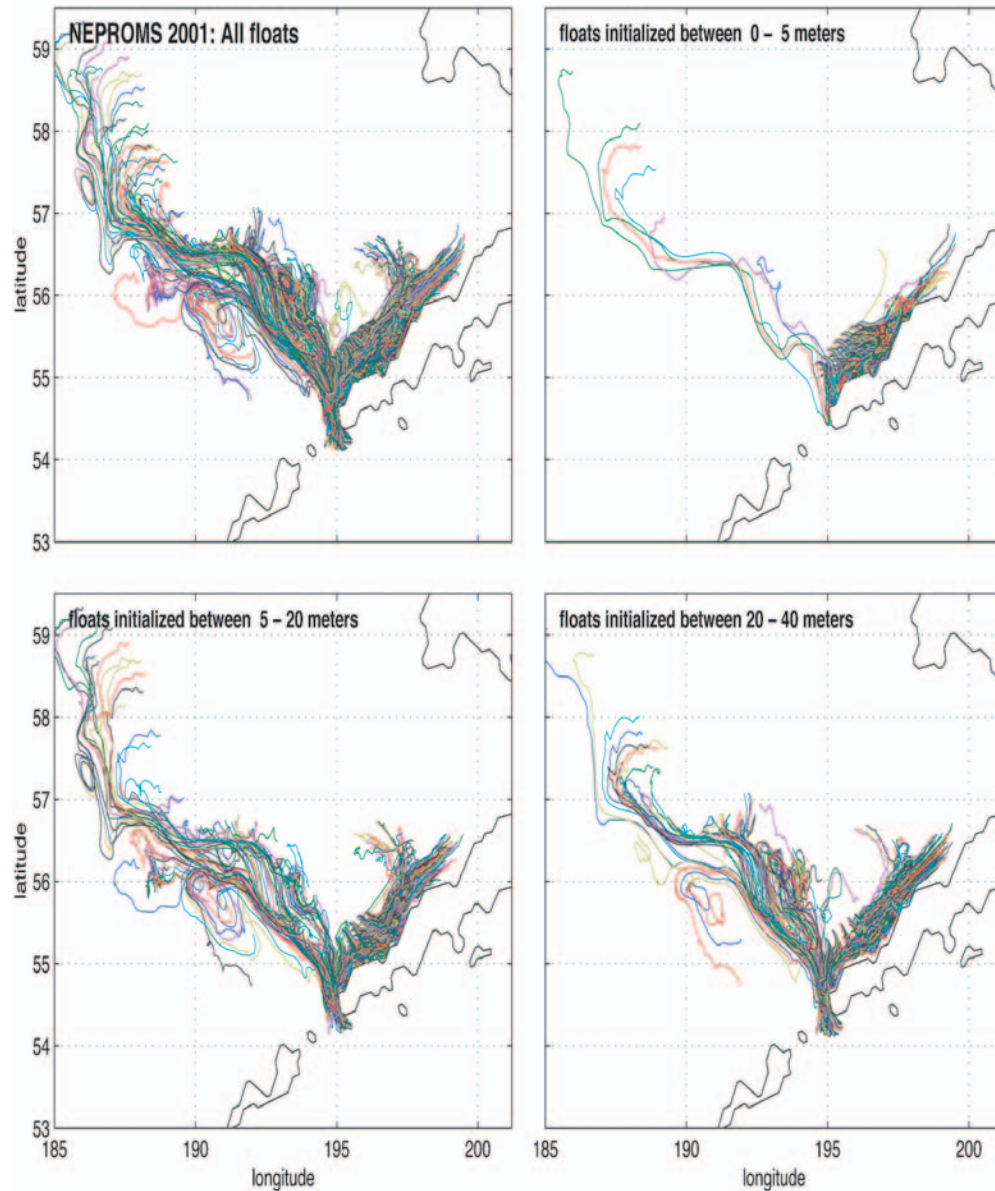


Figure 3.32: Full trajectories for the 2001 90-day simulated drifters. The upper left panel shows all drifters, while the other panels show drifters divided as a function of initial release depth.

in the matrix contain values for that index during that season of each year or links to data that provide values. Not all cells are occupied at this time.

At the bottom of Fig. 3.33 are labeled tabs that represent the spatial dimension of the matrix. The matrix encompasses the same geographic domains that are discussed elsewhere in this document (Section 3.3.4) and described by Hunt *et al.* (2002a). Clicking on a tab brings to the screen an identical grid of indices and years, but the cells are populated with values specific to the region selected.

Besides the indices matrix, there is also a matrix of data available for

Index	1997				1998			
	annual avg	spring bloom	summer	fall ovrtrn	annual avg	spring bloom	summer	fall ovrtrn
Age-0 cannibalism								
Ice retreat		Apr 2				Mar 7		
Last storm		May 15				May 15		
Stratification date		May 1				May 15		
Thermocline depth			20				30	
Thermocline ΔT			11				7	
SST maximum			14				12	
Depth-averaged T_{max}			4.5				6	
PWP stratification		0.7638				1.052		
PWP stratification date		ice				Jun 16		
PWP stratification temperature						2.87		
Slope current	6				2			
Fluorescence peak		Apr 15-30				May 10-?		
Early May nitrate		0 sfc 10 deep				12 sfc 11 deep		
Early May ammonium		8 sfc 10 deep				10 sfc 6 deep		
Copepod $^{*}N$	13.5				10			

Thermocline ΔT : stratification as measured by strength of thermocline ($^{\circ}C$) on Jul 1 (from Henrichs)

Inshore N. Middle Shelf S. Middle Shelf Peninsula N. Outer Shelf Pribilofs S. Outer Shelf Unimak

Figure 3.33: A portion of the SEBSCC indices matrix showing some indices for the South Outer Shelf region during 1997 and 1998.

the Pribilof Islands. This matrix, too, can be found by linking to “Phase III Working Groups” on the SEBSCC web site.

3.4 Application of a Transport and Predation Index to Recruitment for Stock Assessment Purposes (Jim Ianelli)

3.4.1 Background

Recruitment or year-class strength (the numbers of fish successfully surviving larval and post-larval stages, e.g., to age 1) is a fundamental part of the population model used for pollock stock assessments (e.g., Ianelli *et al.*, 1998). The recruitment estimates provide the basis for population numbers that are tracked over time and modified by various natural and fishing mortality sources. The statistical assessment models used in these analyses are similar to state-space models where unknown and unobservable quantities (e.g., numbers of fish) are modeled separately as “state” variables. “Observation” equations are then constructed to translate the state variables into model predictions. These predictions are then compared with actual data to tune the state variables (i.e., the fundamental parameters) using statistical methods such as maximum likelihood. Schnute (1994) provides a good description of this general approach.

Estimates of year-class strengths (e.g., Fig. 3.34) thus are derived from

a variety of information used in the assessment model. This information includes annual bottom-trawl surveys of the entire shelf area (within the U.S. EEZ), bi-annual echo-integration trawl (EIT) surveys of this region, annual fishery catch data from scientific observers aboard fishing vessels, and estimates of biological characteristics (age composition, growth, and maturation, etc.). These assessment analyses lead to recommendations on risk-averse harvest levels for the coming year. The recommendations are influenced by estimates of the underlying stock-recruitment relationship within the integrated assessment model (the so-called stock-recruitment sub-model; Fig. 3.35). Further, the stock-recruitment sub-model can be modified to incorporate environmental indices. Because the framework of the integrated model separates the state dynamics from the observations, it is relatively straightforward to test alternative hypotheses. We illustrate one such modification to evaluate the impact of progressively adding recruitment effects beginning with the simplest form (a mean and deviation) and then additional terms related to the stock size and any environmental terms and process errors. These can be written as recruitment state variables:

$$R = \text{Mean} + \xi, \quad (1)$$

$$R = f(S) + \xi, \quad (2)$$

$$R = f(S) + E, \quad (3)$$

$$R = f(S) + E + \xi, \text{ or} \quad (4)$$

$$R = f(S) + E' + \xi, \quad (5)$$

where R is an actual (unobserved) state variable (log-recruitment) for a given year, and the error term ξ can be thought of as one that encompasses all “natural” variability that is not described by other terms in the above sub-models. For example, sub-model (3) is written such that all recruitment variability is determined by the stock-recruitment function $f(S)$ and an environment term E . This simply means that there is no residual process error in recruitment specifications (i.e., the model terms determine all of the variability in recruitment). For sub-model (5), the conditions for the environment term E' (described below) are “smoothed” with respect to spatial correlation.

In searching for the appropriate environmental term(s), water temperature, turbulence, and transport have been related to success of recruitment for many marine species (e.g., Quinn and Niebauer, 1995). Here, we follow the construct that the transport of planktonic stages is important to establish separation of young pollock from their cannibalistic adults (Wespestad *et al.*, 2000). We used the Ocean Surface Current Simulations (OSCURS) numerical model (Ingraham and Miyahara, 1988) as a means to represent the effective interannual variability of advective egg and larval transport. The model simulates transport trajectories for passive, floating (or near-surface) objects that are propelled by ocean surface currents forced by wind.

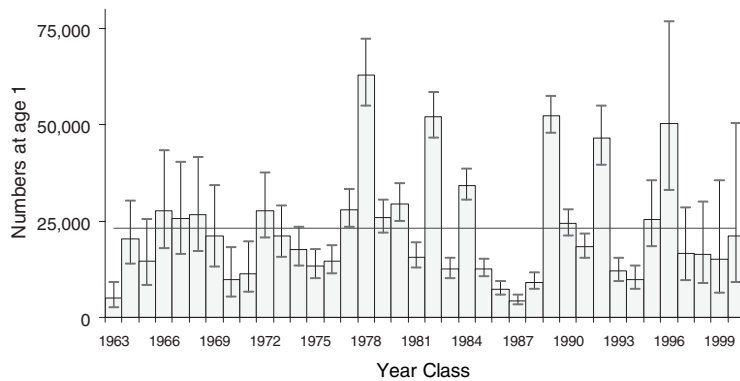


Figure 3.34: Time series of year-class abundance at age 1. Error bars represent approximate 95% univariate confidence bounds. Note that covariance estimates among adjacent year classes is typically highly negatively correlated. Source: Ianelli *et al.* (2001).

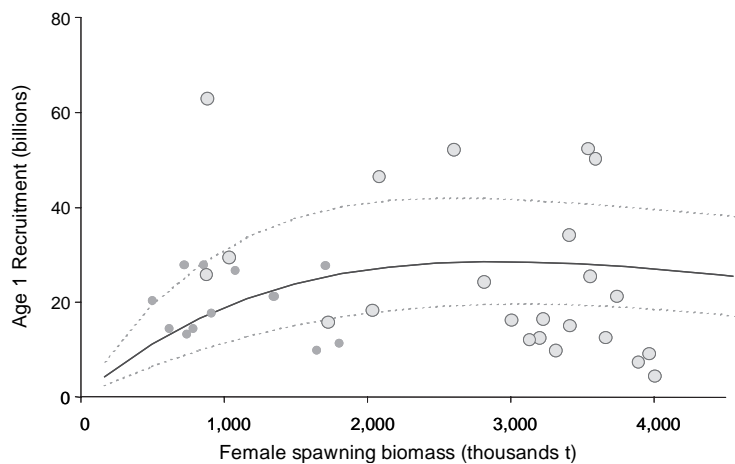


Figure 3.35: Stock-recruitment relationship showing the fitted effect due to spawning biomass (thick line) and estimates from the stock assessment model. Note that the large dots are used to tune the stock-recruitment sub-model while the smaller dots represent points from the regime prior to 1977. Dashed lines represent approximate 95% confidence bands about the curve. Source: Ianelli *et al.* (2001).

3.4.2 An application

The following serves to illustrate one method for incorporating environmental information within an integrated stock assessment approach such as that currently used for EBS pollock. Incorporation of any index can be done in a similar fashion. The integrated assessment model is a good way to evaluate candidate indices because consistency with all available data can be easily evaluated. In addition, compared to methods simply using recruitment residuals, the integrated model provides a more statistically defensible approach as fewer assumptions are required (e.g., analyses of residuals done separately

typically fail to account for the uncertainty of the estimates of the residuals themselves). A disadvantage of the integrated assessment approach is that a fair amount of specialization is required to run the models.

The OSCURS model was run using a single launch site (55.5°N, 165°W) for 90-d trajectories starting 1 April. This location and date were selected based on the distribution and timing of the main concentrations of spawning pollock. The variability of this location appears to be moderate based on the catch-distribution of the fishery for pre-spawning pollock (Fig. 3.36). However, this observed variability is partly attributed to fishing fleet behavior under variable ice conditions and management measures.

Simulations were generated for the years 1964 to 1998 (Fig. 3.37). The endpoints of these trajectories suggest that the young-of-year pollock are either just seaward of the inner front or in the coastal domain as defined in Kachel *et al.* (2002). To quantify the effect these trajectories may have on recruitment success, we chose to compute the average location of the 90-day drifter. The average location represents the characteristics of the advective forces better than the endpoints and reduces the impact of drift outliers (i.e., high-levels of drift over a few days). These average locations were then placed in the context of a grid (Fig. 3.38) in order to geo-reference the advection by year. Each year, therefore, was assigned to a grid-cell (but not all grid-cells had observations). The integrated assessment model was then used to estimate the “effect” a particular grid-cell has relative to recruitment success. In other words, each cell was estimated as being favorable, unfavorable, or neutral to pollock year-class strength.

To make the model well conditioned, two penalty weights were added to the (negative-log) likelihood function. First, a very small grid-cell penalty was added so that for cells with no observations, the estimated recruitment effect would be zero (yet still with the desired high variance). The second (more important) penalty effectively conditions the grid surface values to have a non-parametric surface such that there is some degree of spatial correlation. The value of this penalty weight affects the “smoothness” of the surface by way of multiplying the sums of squared third-differences between grid-cell values in both the lateral and longitudinal directions (Ianelli *et al.*, 1998). In the limit, as the value of this multiplier becomes large, the effect of the grid on explaining recruitment variability goes to zero (i.e., the two-dimensional surface is represented by a single mean value). As the smoothness penalty multiplier tends toward zero, the cells become independent from contiguous (and all other) cells. Alternative values of this multiplier have been explored and are shown in Figs. 3.39a and b. Note that in Fig. 3.39a, the “effect” of larval drift is more irregular compared to the model where smoothness in space is assumed (Fig. 3.39b). Root-mean squared errors of all five sub-models for this application are shown in Table 3.2.

3.4.3 Discussion

For the eastern Bering Sea, wind-driven advection of surface waters containing planktonic stages of pollock (Wespestad *et al.*, 2000) and Tanner crabs (Rosenkranz *et al.*, 2001) appears to account for some of the observed fluctu-

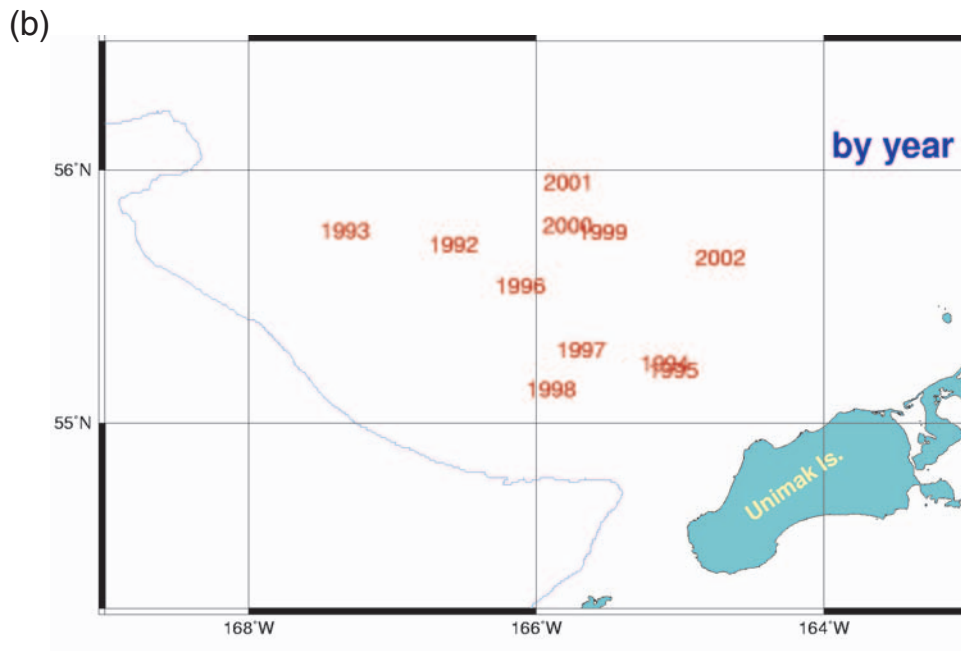
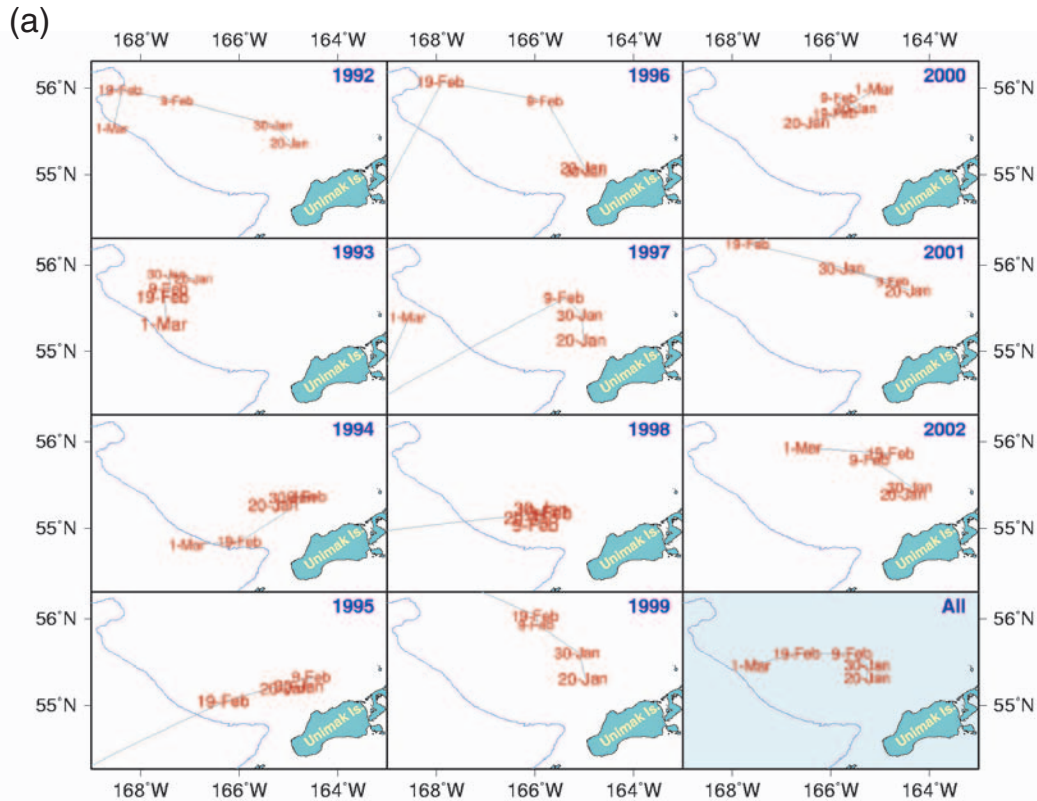


Figure 3.36: Top panel (a): Average catch distribution by 10-day periods, 1992–2002. Bottom right corner is average over all years combined. Bottom panel (b): Average catch distribution of the pollock fleet targeting pre-spawning pollock by year, 20 January–28 February.

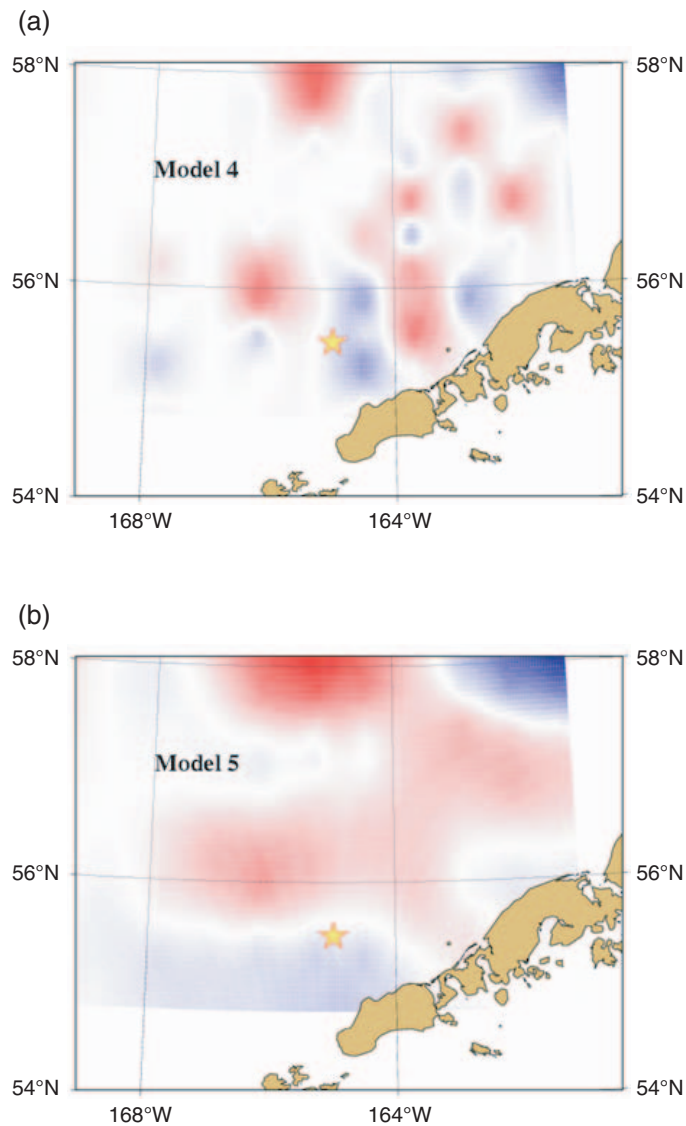


Figure 3.39: Graphical results of fitting a drift component within the integrated stock assessment model. Red areas indicate higher recruitment success while blue represents lower values. Panel (a) is the result for Model 4 (not smoothed) compared with Model 5 (where some degree of spatial correlation is specified).

tuations in year-class strength. In these studies, the biological process that links advection to year-class strength is differential survival.

The role of cannibalism in influencing population dynamics resulting from the strong year class has been examined (Livingston and Methot, 1998). For the age-0 pollock, predation by older pollock can have a strong influence on year-class strength.

A number of caveats exist in the above analysis. For example, the mechanistic model is one that deals with the negative effects of spatial overlap between age-1 juveniles with pollock that are generally older than age 2

Table 3.2: Root-mean squared errors of recruitment sub-model results.

Model component	Model				
	1	2	3	4	5
Mean	0.00	—	—	—	—
Stock-recruitment function, $f(S)$	—	0.04	0.08	0.09	0.09
OSCURS avg. drift	—	—	0.48	0.21	0.11
Residual (ξ)	0.75	0.72	—	0.21	0.28
Total	0.75	0.75	0.56	0.51	0.47

(Fig. 3.40). Analyses of an index of separation (Equation 6) may provide some insight on whether other data are consistent with this process.

$$I_i = \frac{\sum_{\text{all stations}_i}^{n_i} (p_{\text{age}2+} - p_{\text{age}1})^2}{\sqrt{n_i}} \quad (6)$$

where $p_{\text{age}1}$ and $p_{\text{age}2+}$ are the proportions at age 1 and ages 2 and older, respectively. These values were computed at each station sampled during a given survey (Wespestad *et al.*, 2000). Results compared with log-recruitment suggest a very weak relationship between separation index and year-class strength (Fig. 3.41).

Another caveat for this approach is that there are physical and biological assumptions imbedded in how accurately OSCURS simulates the actual transport of pollock eggs and larvae. From a purely physical perspective, we accept that OSCURS is a surface wind-drift model most applicable to approximately the upper 10 m of the water column and to regions where the ambient subtidal currents are weak. For much of the southeastern shelf, the climatological mean currents are weak, yet more active flow has been observed along the 100-m isobath and over the outer shelf/slope (Schumacher and Stabeno, 1998; Reed and Stabeno, 1996; Reed, 1999; Stabeno *et al.*, 2001). One solution is to compare the results from OSCURS to those from more sophisticated hydrodynamic models. Early indications suggest that there is good agreement, except in areas where depth dynamics are particularly acute, e.g., around the Pribilof Islands.

From a purely biological perspective, the question of location of planktonic stages in the water column, and selection of a single launch site must be examined. We show some indication of interannual variability of spawning location (Fig. 3.36) that may be useful to improve launch-site locations. Additionally, multiple launch sites in space and time may also better represent the effect of advection on pollock eggs and larvae. While extensive work has not been conducted on the vertical location of eggs and larvae, over the shelf, larvae do exist in the upper 10 m, but they are often found at greater depths (Napp *et al.*, 2000). This raises the question on what fraction of the planktonic life history stages would follow the wind-drift.

Spawning also occurs near Bogoslof Island and other locations over the

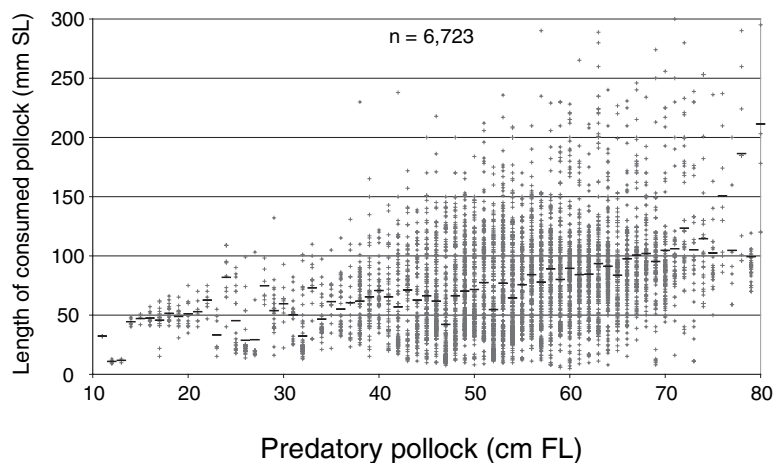


Figure 3.40: Length of pollock consumed compared to the length of the consuming pollock based on NMFS food-habits studies (Troy Buckley, NOAA/AFSC, personal communication).

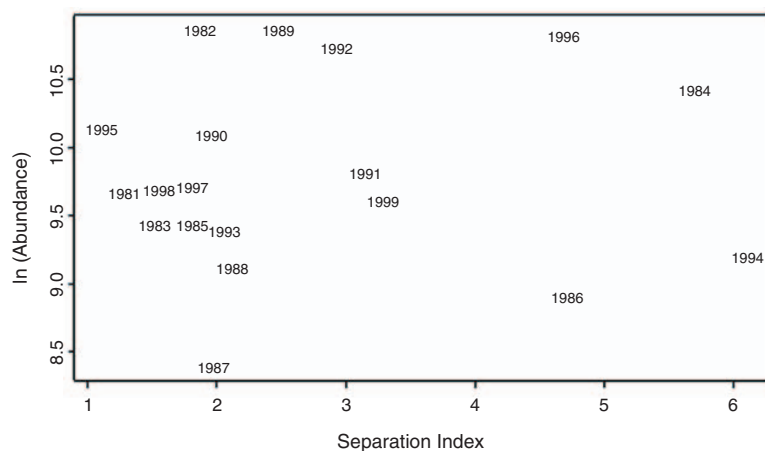


Figure 3.41: Separation index relative to estimates of the log-pollock abundance at age 1, 1982–1999. Numbers plotted represent year-class.

slope and basin of the eastern Bering Sea. These regions were hypothesized to be a source of larvae for the southeastern shelf (Francis and Bailey, 1983). If significant spawning occurs off the shelf where high concentrations of larvae have been observed (Schumacher and Stabeno, 1994), then the simple set of initial conditions for the drift-effect on recruitment are further complicated. It appears that larvae in these waters are likely to be deeper in the water column (Napp *et al.*, 2000) and the background currents are typically stronger than over the middle shelf (Stabeno *et al.*, 1999a). Alternative drift locations to represent the starting points of egg and larval stages may require further exploration, particularly if there is a significant amount of pollock egg production from the Aleutian basin region.

3.5 Changing Relationships between Climate and Biological Indices in the Eastern Bering Sea (Alan Springer)

3.5.1 Introduction

Climate change, whether considered at local or global spatial scales and annual or millennial time scales, is among the most controversial and intriguing environmental issues confronting us today. The obvious concerns over climate change are effects it has on ecosystem structure and function, food web productivity, the abundance of individual species, and the economies and livelihoods of people the world over.

Nowhere have the effects of climate change on marine ecosystems been better documented than in the North Pacific Ocean (e.g., McGowan, 1990; Ebbesmeyer *et al.*, 1991; Beamish, 1995; Mantua *et al.*, 1997; Francis *et al.*, 1998; Klyashtorin and Rukhlov, 1998; Springer, 1998; Welch *et al.*, 1998; Anderson and Piatt, 1999; Hare *et al.*, 1999; Hare and Mantua, 2000). The common approach in most analyses of climate and other ecosystem components has been to compare slopes of parameter values over time, slopes that change when the climate changes from one quasi-stable state, or regime, to another. Regime shifts are defined by abrupt, sustained polarity reversals of the Pacific Decadal Oscillation (PDO) (Trenberth and Hurrell, 1994; Mantua *et al.*, 1997).

In contrast, there have been comparatively few analyses of relationships between two variables when time was not one of them. In order to better understand ecosystem processes that respond to climate change and regime shifts, it would be helpful to have correlations between things that are, or might be, functionally related. For example, correlations between fluctuations in primary physical forcing parameters, such as the Aleutian Low pressure field, and some response variables, such as wind, mixing depth, and primary productivity, as was modeled for the Gulf of Alaska by Polovina *et al.* (1995); and temperature and zooplankton population dynamics in the Gulf of Alaska (Mackas *et al.*, 1998).

A small assortment of data sets for the Bering Sea can be grouped in ways that yield marginally miscellaneous and eclectic, but compelling, relationships. These relationships provide insight into time and space scales of interest and the sensitivity of ecosystem components and processes to climate change. This includes changes in the general climate state, e.g., PDO, and to interannual fluctuations in climate within and across regimes. Some of the relationships are between adjacent ecosystem elements that could be thought of as functional cause and effect relationships. Other relationships are separated by more than one element. Such ostensibly functional relationships are useful to know, even if the variables are separated by more than one trophic level, since they may give clues about where and how to look for processes responsible for biomass yield at any trophic level.

3.5.2 Observations

The time series used to develop and examine potential relationships are:

- a. North Pacific Index (NPI)—area averaged mean sea level pressure anomaly over the region 30° to 65°N, 160°E to 140°W (Trenberth and Hurrell, 1994; Minobe, 1999);
- b. Sea surface temperature (SST)—mean temperature of a 5° × 5° block centered on (55°N, 170°W) (Cayan, unpublished data);
- c. Bering Sea wind measured at St. Paul Island by the U.S. National Weather Service (Note, the wind speed has been cubed so that it provides an index of mixing.);
- d. Sea-ice coverage over the eastern Bering-Chukchi shelf (Niebauer, 1998 and unpublished data);
- e. Bering Strait transport—annual northward transport through Bering Strait (Roach *et al.*, 1995; T. Weingartner, unpublished data);
- f. Global ocean temperature (NCDC, 2004);
- g. Bowhead whale baleen stable carbon isotope ratios ($\delta^{13}\text{C}$) (Schell, 2000);
- h. Steller sea lion abundance (NMML, 1994 and unpublished data; Trites and Larkin, 1996);
- i. Age-1 pollock abundance and age-3+ pollock biomass (J. Ianelli, unpublished data);
- j. Red-legged kittiwake productivity at St. George Island, Pribilof Islands (Dragoo *et al.*, 2001);
- k. Seabird abundance at the Pribilof Islands and Aleutian Islands (Dragoo *et al.*, 2001);
- l. Fur seal pup production on St. Paul Island, Pribilof Islands (York and Hartley, 1981; York and Kozloff, 1987; A. York, unpublished data);
- m. Fur seal growth rates (A. Trites, unpublished data); and
- n. Common murre and thick-billed murres relative abundance at Walrus Island, Pribilof Islands (Peterson and Fisher, 1955).

3.5.3 *Physical-physical relationships*

Despite considerable uncertainty about the relative importance of processes governing community structure and the abundances of individual species, e.g., top-down versus bottom-up interactions, much which transpires in ecosystems begins with physics. Francis *et al.* (1998) have presented a conceptual model of the pathways by which changes in atmospheric features can influence biota, and Schumacher *et al.* (2003) have modified this model for the Bering Sea (Fig. 3.3). Both of these models show that physics can influence an ecosystem in either top down or bottom up modes. For the North Pacific and eastern Bering Sea, much of the physics begins with the Aleutian Low pressure system that can be scaled by the North Pacific Index (NPI).

Winter sea ice extent and duration in the Bering Sea are related at the decadal scale to mean atmospheric forcing (Niebauer, 1998; Wyllie-Echeverria and Wooster, 1998; Stabeno *et al.*, 2001). Sea ice influences the ecosystem through at least two pathways. First, the presence of sea over the southeastern shelf in March (when ambient light is adequate to sustain primary production) can result in an early phytoplankton bloom (Stabeno *et al.*, 1998). An early bloom may result in a greater energy flow to the benthic community, whereas a bloom later in spring likely favors pelagic pathways (Walsh and McRoy, 1986; Hunt *et al.*, 2002a). The extent of sea ice is also vital to the subsequent development of the middle shelf cold pool that appears to influence the distribution of pollock and Arctic cod. The timing and magnitude of the summer retreat of sea ice is related to summer climate, which can be indexed by the NPI (Fig. 3.42). Recent results indicate that regions of the Bering Sea have shifted toward an earlier spring transition (Stabeno and Overland, 2001). The retreat and melting of sea ice also have ecosystem effects as they alter the availability and distribution of essential habitat for symphagic food webs and pagophilic marine mammals. In addition, they are related to energy flow through the ecosystem as noted above.

One of the hallmark features of the Bering Sea is the transport of water north through Bering Strait into the Chukchi Sea. This transport occurs because of differential atmospheric pressure across the western Arctic that tilts sea level down toward the north (Coachman *et al.*, 1975). Not surprisingly, then, variability in annual transport is related to variability in atmospheric pressure, as reflected again by the NPI (Fig. 3.43). A long-term decline in the mean strength of the Aleutian Low may explain the decline in transport in the past five decades. This, in turn, would be expected to have a large effect on production budgets across the northern Bering-Chukchi shelf, because nutrients and biota carried in the current transform the region into one of the most highly productive regions in the world (Springer *et al.*, 1989; Springer and McRoy, 1993).

Wind measured at St. Paul Island is related to the atmospheric pressure field (Fig. 3.44). The dramatic drop in the mean winds during the mid-1970s to late 1980s corresponded to a similar change in the NPI and to a pronounced increase in average global ocean temperature (Fig. 3.45).

St. Paul wind is also related to ocean temperature in the Bering Sea (Fig. 3.46). However, the correlation is only apparent within a given regime and changes from one regime to the next. That is, wind and SST were generally out of phase prior to 1977, were generally in phase between 1977 and 1989, and then generally out of phase again after 1989. Interannual fluctuations in wind and SST are not always proportional, indicating, not surprisingly, that other factors are important in determining magnitudes of the two variables.

3.5.4 Physical-biological relationships

Carbon stable isotope ratios ($\delta^{13}\text{C}$) of baleen from bowhead whales exhibit considerable interannual variation since the late 1940s, including a

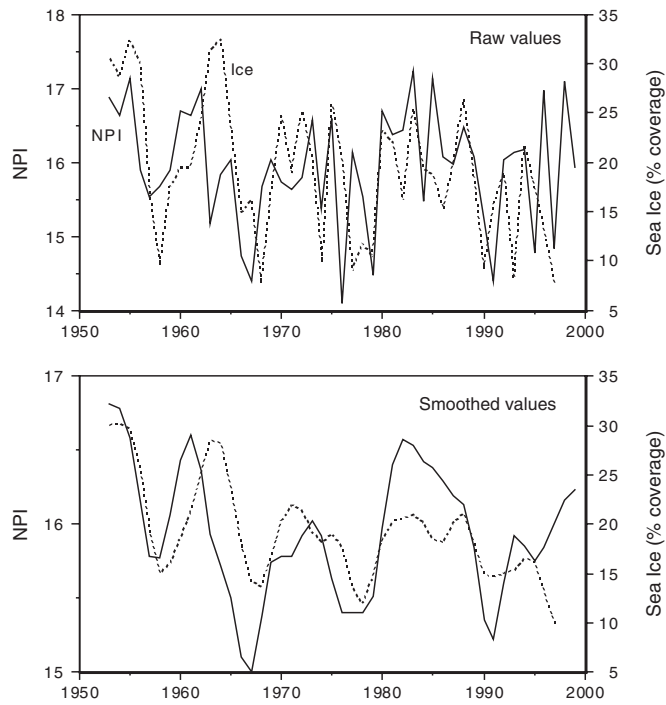


Figure 3.42: Summer extent of sea ice scaled as percent coverage of the Chukchi-Bering shelf (see Niebauer, 1998) and mean July–September NPI.

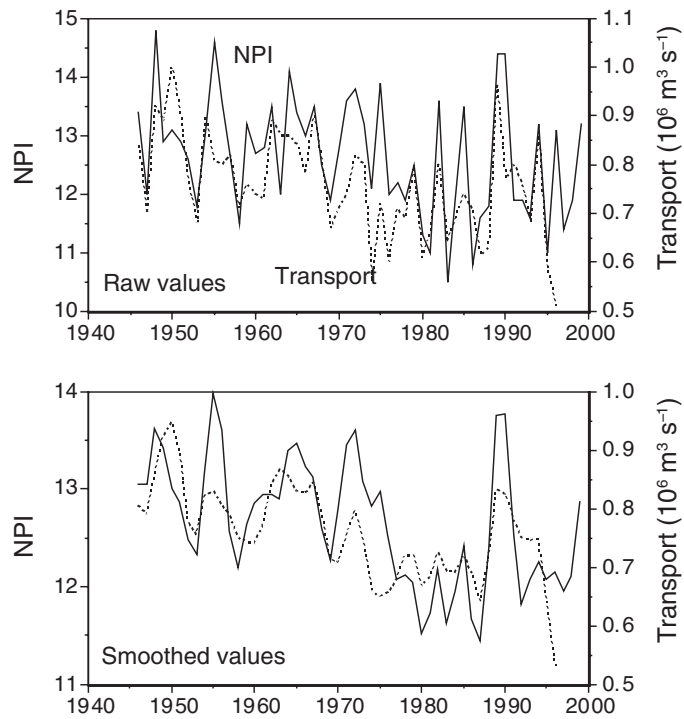


Figure 3.43: Annual northward transport through Bering Strait and the mean annual NPI.

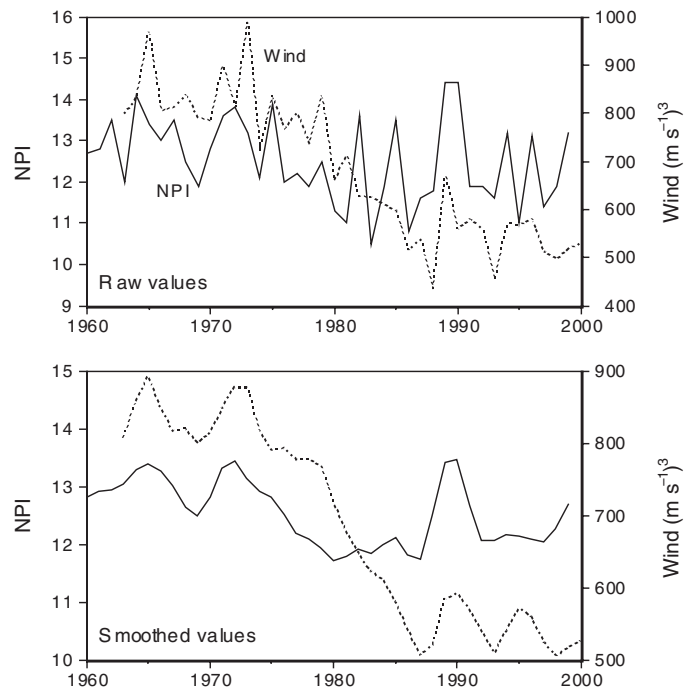


Figure 3.44: Mean annual wind at St. Paul and the NPI.

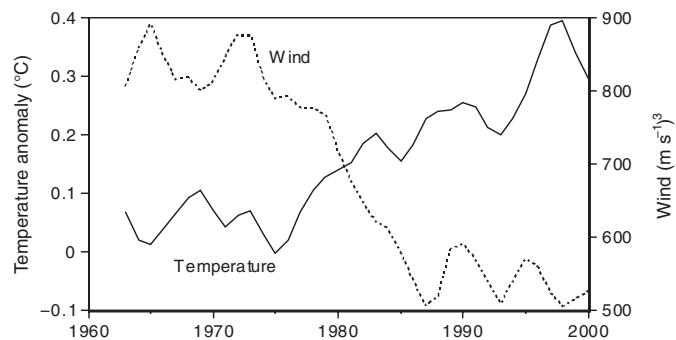


Figure 3.45: Mean annual wind at St. Paul and the global ocean temperature anomaly. Wind data smoothed.

pronounced overall shift that has been proposed as evidence of a decline in primary productivity of some 30% in the Bering Sea (Schell, 2000). The pattern in baleen $\delta^{13}\text{C}$ variability matches the pattern in winds over the same interval when baleen is lagged by 1 year to account for the ecological separation between whales and physical forcing (Fig. 3.47).

Wind also is correlated in a general way with sea lion abundance at several colonies in the Bering Sea range of the endangered western stock (Fig. 3.48). That is, sea lion abundance declined abruptly and precipitously at the same time that winds declined in a similar manner in the Bering Sea.

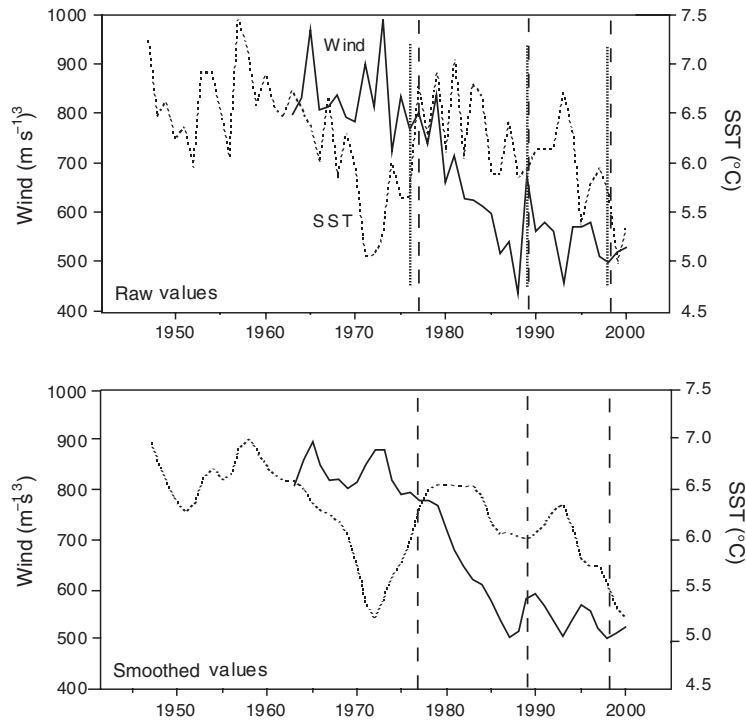


Figure 3.46: Mean annual wind at St. Paul and sea surface temperature (SST) in the eastern Bering Sea. Vertical lines show regime shifts in 1977, 1989, and 1998.

Sea surface temperature (SST) has varied since the late 1940s and is highly correlated with at least four biological variables in the Bering Sea: the abundance of age-1 pollock, the biomass of age-3+ pollock, and the productivity of black-legged and red-legged kittiwakes on the Pribilof Islands. However, except for age-3+ pollock biomass, the correlations exist only within regimes as defined by the PDO, where they are very strong but have alternating signs from regime to regime (Figs. 3.49, 3.50). Pollock biomass was positively correlated with spring SST for 25 years when SST is lagged by four years to account for separation between given SST years and the integrated effect expressed in the pollock age classes where most biomass resides (Fig. 3.51). Does the 4-year lag also suggest that most of the impact of SST (or for whatever it is surrogate) on pollock populations occurs between egg and age-0 fish? If so, one could infer many possible pathways from the correlation.

3.5.5 Biological-biological relationships

The most conspicuous correlations between biological variables in the Bering Sea are trends in abundances of piscivorous seabirds and fur seals on St. Paul Island and St. George Island (Pribilof Islands) and Bogoslof Island and Buldir Island in the Aleutian Islands (Table 3.3). Trends are uniformly negative on St. Paul and uniformly positive on Bogoslof and Buldir. On St. George, both species of kittiwake and fur seals are declining as at St.

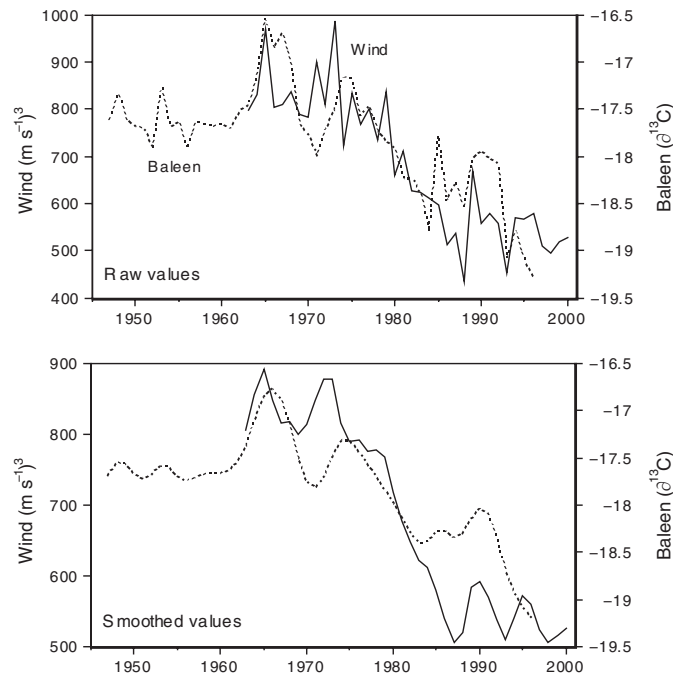


Figure 3.47: Bowhead whale baleen $\delta^{13}\text{C}$ (lagged 1 year) and mean annual wind at St. Paul.

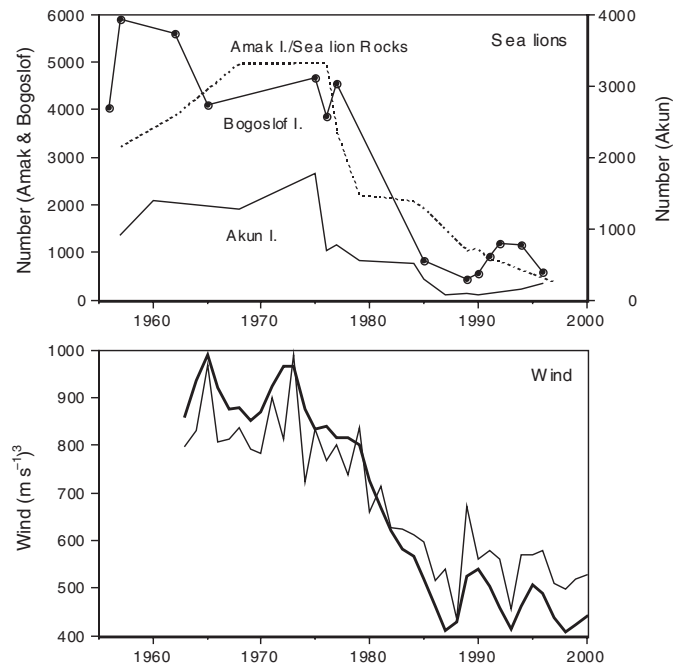


Figure 3.48: Sea lion abundance at rookeries in the eastern Aleutian Islands and wind at St. Paul Island. Heavy line in wind panel is the smoothed trend.

Table 3.3: Trends in populations of seabirds and fur seals at four locations in the Bering Sea.

Location	Species	Interval	n	% Change	r ²
St. Paul I. (<i>Pribilofs</i>)	Black-legged Kittiwake	1976–1999	12	–73	0.79
	Red-legged Kittiwake	1976–1999	12	–70	0.72
	Common Murre	1976–1999	12	–62	0.62
	Thick-billed Murre	1976–1999	12	–44	0.72
	Northern Fur Seal	1975–2000	24	–37	0.6
	Mean (SE)				–57 (7.1)
St. George I. (<i>Pribilofs</i>)	Black-legged Kittiwake	1976–1999	11	–47	0.45
	Red-legged Kittiwake	1976–1999	11	–52	0.63
	Common Murre	1976–1999	11	+55	0.56
	Thick-billed Murre	1976–1999	11	0	—
	Northern Fur Seal	1975–2000	24	–70	0.84
	Mean (SE)				–23 (23)
Bogoslof I. (<i>E Aleutians</i>)	Black-legged Kittiwake	1973–2000	3	+150	0.8
	Red-legged Kittiwake	1973–2000	3	+550	0.95
	Tufted Puffin	1973–2000	5	+130	0.98
	Northern Fur Seal	1980–1997	12	+2500	0.98
	Mean (SE)				+832 (564)
Buldir I. (<i>W Aleutians</i>)	Black-legged Kittiwake	1974–1996	10	+450	0.84
	Red-legged Kittiwake	1974–1996	10	+200	0.81
	Thick-billed Murre	1974–1996	10	+320	0.91
	Mean (SE)				+323 (72)

Paul. Thick-billed murres declined through the 1980s but have increased since then, whereas common murres increased throughout this period. All of these species are supported by a common suite of pelagic forage fishes and squids that includes prominently juvenile pollock at the Pribilof Islands.

There is an obvious similarity between the pattern of change in fur seal numbers at St. Paul—a prolonged decline punctuated by intervals of increase—and the pattern of change in $\delta^{13}\text{C}$ of bowhead whale baleen (Fig. 3.52). Were it not for the overriding effect of the female harvest on population stability in the period 1956–1968 (York and Hartley, 1981), the response of fur seals to an apparent environmental signal might have been stronger. That is, the increasing trend in numbers in the mid-1960s may have been attenuated by pressure on the population from excessive female harvests. Otherwise, fur seal pup production and bowhead baleen seem to be recording events that originate with fluctuations in climate and propagate through the system.

Additional evidence of the sensitivity of fur seals to ecosystem state is found in patterns of growth in body size over time. In the past century, fur seals on St. Paul experienced periods of faster and slower growth (A. Trites, unpublished data), with each period lasting about as long as a climate regime

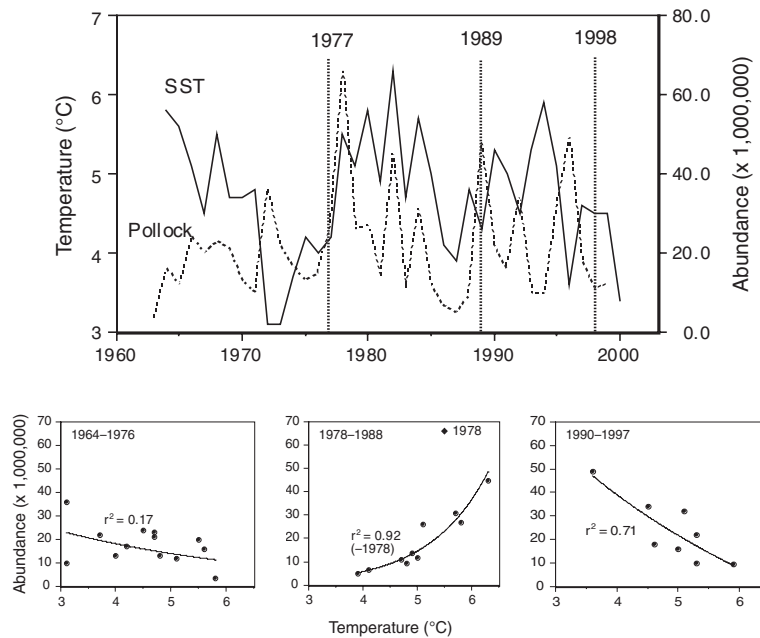


Figure 3.49: Abundance of age-1+ pollock and mean April–June sea surface temperature (SST: lagged 1 year) on the eastern Bering Sea shelf. The transition years (1977, 1989, and 1998) are not included in the regression, nor is 1978, as it was an extreme in recruitment.

(Fig. 3.53). Faster growth occurred in regimes when common murrens apparently predominated at Walrus Island, a small island in the Pribilof group where murrens once nested in immense numbers: murrens were eliminated by foxes that gained access to the island over winter ice in the early 1970s. Conversely, slow growth occurred in regimes when thick-billed murrens apparently predominated. The well-documented alternation between murre species on Walrus Island (Peterson and Fisher, 1955) also corresponded to shifts in climate regime (Springer, 1998).

Fur seals are ecologically more similar to common murrens than to thick-billed murrens. That is, fur seals and common murrens are more dependent on pelagic prey, whereas thick-billed murrens incorporate a significant amount of benthic prey in their diets (Springer, 1991; Sinclair *et al.*, 1994; Springer *et al.*, 1996). Therefore, the correspondence of positive responses of fur seals and common murrens during periods when thick-billed murrens apparently responded negatively is theoretically tractable.

3.5.6 Discussion

Functional relationships should typically have just one sign—positive or negative. Among the examples presented here, it is reasonable to believe that the common pattern of variability in meteorological conditions, as indexed by the NPI, and regional wind (observed at St. Paul) represents a positive functional forcing-response relationship over the Bering Sea. It further can be

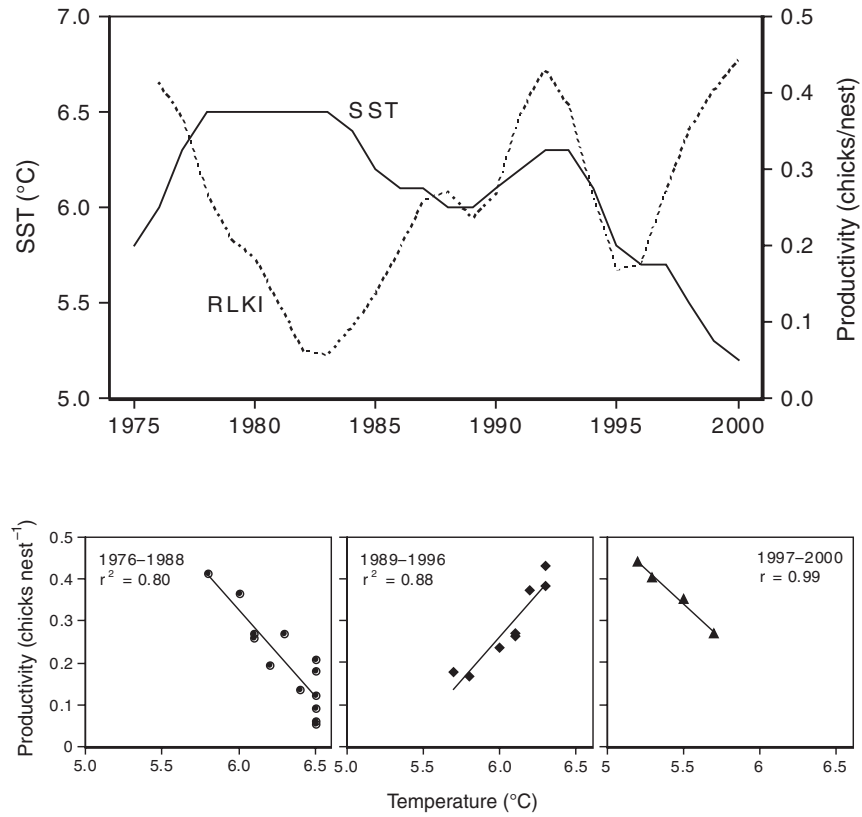


Figure 3.50: Red-legged kittiwake productivity at St. George Island and mean annual sea surface temperature (SST) in the eastern Bering Sea. Smoothed trends. A similar relationship exists for black-legged kittiwakes.

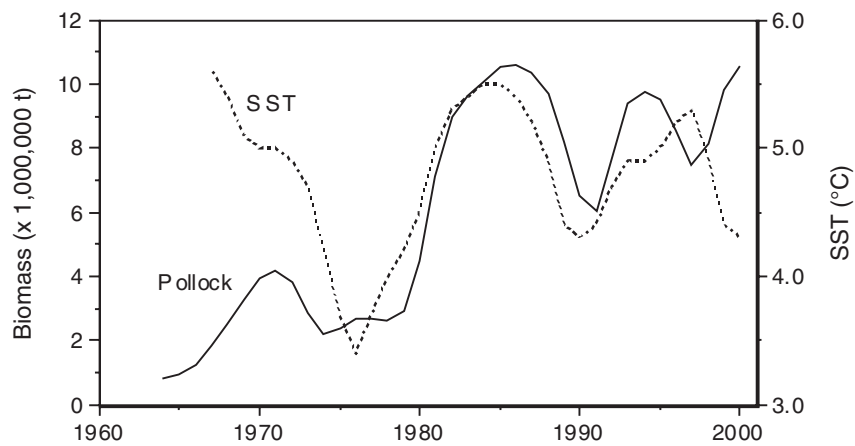


Figure 3.51: Biomass of age 3+ pollock in the eastern Bering Sea and mean April–June sea surface temperature (SST: lagged 4 years). Smoothed trends.

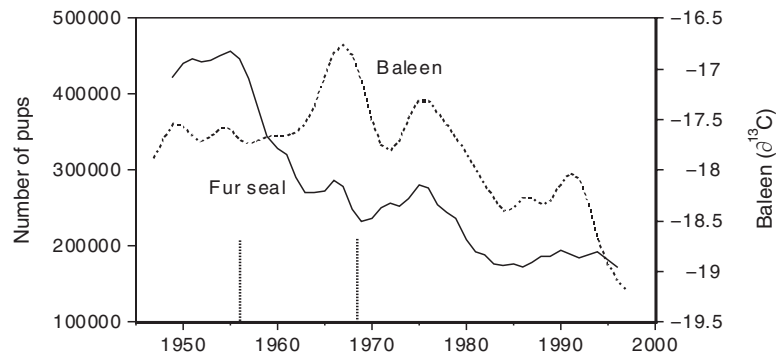


Figure 3.52: Fur seal pup production on St. Paul Island and isotope ratios in bowhead whale baleen. Smoothed trends. Dotted vertical lines at 1956 and 1968 mark interval of experimental female harvest.

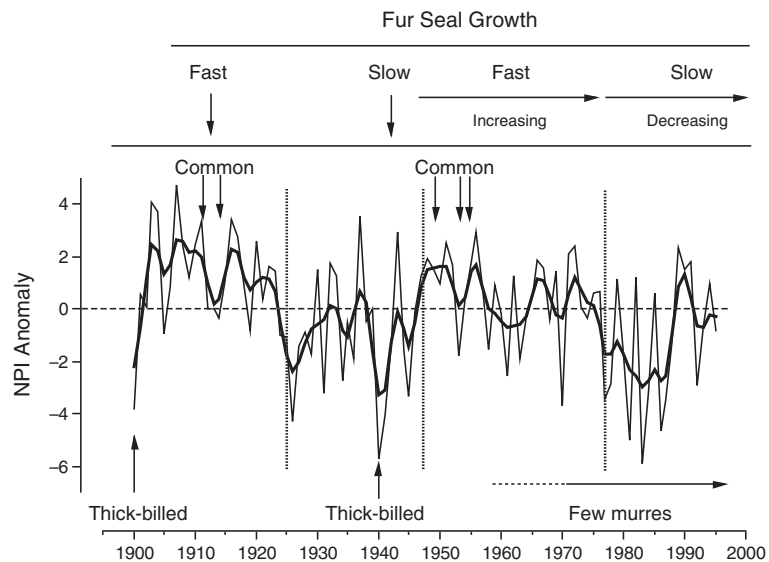


Figure 3.53: Fur seal growth at St. Paul Island and the relative abundance of common and thick-billed murrens on Walrus Island. Dotted vertical lines mark regime shifts in 1925, 1947, and 1977 (Mantua *et al.*, 1997). Adapted from Springer (1998). Heavy line is smoothed trend.

argued that basin-scale meteorology and thus regional winds are influenced by changes in mean characteristics of the global-scale ocean-atmosphere interactions. Variability in the Aleutian Low and elements of physical oceanography, such as transport through Bering Strait and the summer retreat of sea ice in the Chukchi Sea, must represent positive functional forcing-response relationships across the atmosphere-ocean interface.

In contrast to these single sign relationships, the sign of the relationship between wind and SST in the Bering Sea has alternated between generally negative and generally positive depending upon regime. A negative relation-

ship might always be expected, since during much of the year wind mixes the upper layers of the ocean, countering effects of stratification and surface heating from the sun. Thus, it appears that while wind and SST in the Bering Sea may be adjacent ecosystem elements under certain conditions, under other conditions they may be separated by one or more other elements. Alternatively, it may be that under certain conditions, another element overrides the likely role of wind on SST, or perhaps wind and SST are responding independently to some other feature(s) of the physical system.

Similarly, it appears that the relationship between summer atmospheric forcing and summer retreat of sea ice was generally in phase during the 1950s through 1980s, but has been out of phase since. This may also represent the influence of another element dominating sea ice extent, e.g., an interaction with the Arctic Oscillation. Even during the long interval of positive correlation, the pattern of the NPI did not always exactly match that of summer sea ice extent, further implicating other factors in the full equation.

Biological variability should reflect physical variability. In the Bering Sea, the 50-y time series of $\delta^{13}\text{C}$ in bowhead whale baleen, an ostensible proxy of primary productivity, is well correlated with the NPI and wind. At least two processes could explain these relationships, both of which begin with meteorology. One is that baleen $\delta^{13}\text{C}$ is mediated by wind, which plays major roles in primary and secondary production by creating turbulence that affects mixed layer and nutrient dynamics and feeding efficiencies of planktonic organisms and micronekton. Wind is clearly important to primary production in the Bering Sea (Sambrotto and Goering, 1983; Sambrotto *et al.*, 1986). Another possibility is the effect of atmospheric pressure on transport across the northern Bering-Chukchi shelf, where bowheads obtain the bulk of their annual nutrition (Lee, 2000). Variability in northward transport leads to variability in primary production and the rate of advective supply of zooplankton (Springer *et al.*, 1989; Springer and McRoy, 1993) that might be reflected in the $\delta^{13}\text{C}$ of bowhead baleen.

Members of two contrasting food webs—deep basin pelagic (red-legged kittiwakes) and continental shelf pelagic (black-legged kittiwakes and juvenile pollock)—are extremely influenced by whatever it is that SST indexes. The most intriguing aspect of this is that the sign of the relationship between SST and juvenile pollock and kittiwakes changes between regimes, just as it does with SST and wind. These correlations probably should not be considered functional relationships in the strict sense, since there are potentially several ecological levels that are a bridge between them. It is more likely that SST serves as a proxy for one or more other features of the ecosystem (that change in fundamental ways between regimes relative to SST) that are responsible for the variability in abundance and productivity of the birds and pollock. Still, in a predictive sense, SST is a powerful index provided one knows when a regime shifts.

SST was strongly predictive of age-3+ pollock biomass on the eastern shelf for over two decades, and the sign was always positive regardless of regime, i.e., it did not change after 1989. The significance of the apparently negative relationship in the 1960s is unclear because of the uncertain effect of the rapidly developing commercial fishery on the relatively small virgin

stock. However, the relationship may have again become negative since the mid 1990s. The reason for differences between trends in abundance of juvenile pollock and biomass of adult pollock in relation to trends in SST and regime are not readily apparent.

Just as signs of several relationships change over time as regimes shift, signs of trends in the abundance of seabirds and fur seals vary between habitats within regimes (Pribilof and continental shelf regions vs. Bogoslof and oceanic regions), and ratios of congeneric murre on Walrus Island and growth rates of fur seals vary within habitat between regimes. In the case of fur seal growth rates, the effect is apparently manifested in the Gulf of Alaska as the seals return to the Bering Sea in spring (Trites and Bigg, 1996). The geographic distance between locations where fur seal annual growth is determined and where various parameters are measured in the Bering and Chukchi seas illustrates the spatial scale of influence of an overriding physical forcing factor, which is most likely the Aleutian Low pressure system.

In aggregate, there are numerous correlations among a variety of ecosystem components from fundamental meteorological forcing (the Aleutian Low pressure system) to primary physical response factors (winds, currents, and SST), to secondary physical and biological response parameters (sea ice extent, surrogate primary productivity, and the abundances and productivity of planktivorous fish and piscivorous marine birds and mammals). None of the physical-physical or physical-biological correlations proves cause and effect, but a considerable weight of evidence indicates that climate and climate change are extremely important in regulating production regimes in the Bering Sea. Routes through the ecosystem taken by these supposed chains of cause and effect are conjectural still, but several plausible scenarios come to mind. For example, fluctuating atmospheric pressure affects winds and currents that alter sea ice extent and primary productivity (as indexed by isotope ratios in bowhead baleen). Variable food web productivity, arising from the effect of wind on primary productivity or on transfer efficiencies at low trophic levels, would be important at high trophic levels and could be expressed in fur seal growth, sea lion abundance, and alternating dominance of one or the other species of murre at Walrus Island. The biological-biological correlations presented here demonstrate common responses to signals propagating through the ecosystem, rather than functional cause and effect relationships.

The emphasis of most recent analyses of effects of climate change has been on comparisons of mean parameter values or slopes, e.g., relatively higher or lower atmospheric pressure or increasing or decreasing abundance of a species, between regimes. That is, a given parameter in a given regime is reduced to a single value or sign (positive or negative). The data sets presented here show, in addition, a considerable amount of interannual coherence within and across regimes, supporting the notion that several may involve functional forcing-response relationships. Still, none of the supposed independent forcing variables, e.g., the summer atmospheric pressure field, explains all of the variability in the dependent response variables, e.g., summer sea ice retreat. In all cases, multiple forcing factors are at play.

Many things can affect any parameter's value within a given year, such

as measurement error and random events in the ecosystem. These can be important, for example as when a severe summer storm with high wind and heavy rain blows and washes away seabird chicks from nests, radically lowering productivity from a level that otherwise could have been supported by the system. Such random events are commonly unrelated to fundamental trends in forcing factors and can blur the picture of fundamental form. Thus, for example, the fundamental waveform of the longer-term oscillation of summer NPI and sea ice, irrespective of regimes, can be more clearly seen when the data are smoothed as in Fig. 3.42.

The relationships presented here implicate bottom-up control of various processes linking the Aleutian Low to seabirds and marine mammals. However, this should not be construed to mean that all demographic changes at high trophic levels represent responses to changing food web production and the availability of prey to responding species. In the case of fur seals, for example, variable growth rates likely do reflect changing prey abundance: declining pup production could be caused by declining carrying capacity affecting the ability of females to produce pups, or by the loss of females brought on by starvation (a prey issue) or by predation. That species are sensitive to fluctuations in productivity of supporting food webs is not surprising, nor is it surprising that they are sensitive to changes in predation that might result from, or be exacerbated by, the same bottom-up pathways.

The tendency for the Bering Sea ecosystem to behave in particular ways depending upon seasonal, annual, and mean decadal physical forcing also is not surprising and is evident in numerous time series. What is less intuitive are explanations of the changing signs of relationships between elements of the ecosystem from one climate regime to another, such as between wind and SST and between SST and the productivity of pollock and kittiwakes. In all of these examples, other ecosystem elements must be involved in the actual functional relationships. Nevertheless, it is puzzling how the signs of these relationships change between positive and negative as climate regimes change. Whatever the explanation may prove to be, in the meantime it is important to be mindful of the potential for inconstant polarity, relative not only to time but to other ecosystem attributes. It is especially important when attempting to develop ways to predict an outcome, such as pollock production, based on one or a combination of indices. Ecosystems apparently do have memory, or inertia, but the path taken by ecosystem processes is steered in different directions under different climate situations, thus changing outcomes in ways that are surprising and unpredictable.

3.6 Summary

3.6.1 *Progress accomplished in the development of indices*

The goal of the IWG was to identify potential single- or multi-parameter constructs or indices that lead to development of survival indices for pollock in the early life history stages, and that this information would provide input to the National Marine Fisheries Service (NMFS) in stock assessment of juvenile pollock for use by fisheries scientists at the Alaska Fisheries Sci-

ence Center (AFSC)/NMFS. Toward attaining this goal, extensive progress was made in the development of indices (Table 3.1). The conceptual switch model (Fig. 3.2) developed during SEBSCC Phase I was expanded to include timing of prey production (that, in turn, is related to the presence of sea ice) for first feeding survival, thereby becoming a more complete mirror of the natural ecosystem. The development of an index of mixed-layer characteristics (see Section 3.3.1) provided input to the development of the Oscillating Control Hypothesis (Hunt *et al.*, 2002a). This index of the physical environment, however, does not account for the observed variability in age-1 pollock year-class strength. An index of wind turbulence versus larval feeding success was developed (see Section 3.3.2). The project ended, however, prior to developing a time history of this index to compare with recruitment estimates. For the first time in Bering Sea studies, variations in net short wave radiation were considered as an index (Section 3.3.3). The importance of such variations is only now being recognized world wide as a crucial aspect of time varying forcing for climate and ecosystem change (e.g., Foukal, 2003). A new index of sea ice was developed that led to new insight regarding changes in timing of spring in the region (Stabeno and Overland, 2001). The compilation of water temperature data from the annual trawl survey (Section 3.3.5) now permits further development of indices related to thermal conditions. The model simulations (Section 3.3.6) show that surface wind drift is not sufficient for simulating pollock egg and larval drift. The use of NEPROMS to generate annual drift trajectories requires further funding. A technique was developed that combines early life history transport and predation by adult pollock (Section 3.4). This technique has been transferred to NMFS and is an operational element of the annual stock assessment. Further application of this technique awaits the use of more realistic transport simulations. An examination of a large set of biological and physical indices showed that potential relationships could change sign with regime shifts (Section 3.5), providing a clear warning that a simple linear solution does not exist. The IWG concluded its deliberations by generating a set of indices-related topics that need to be examined (Section 3.6.2), and tools that need to be developed (Section 3.6.3).

The vast quantity of information collected during SEBSCC has led to new understanding and hypotheses of how the southeastern Bering Sea ecosystem functions. This information is providing input to the National Marine Fisheries Service's stock assessment of juvenile pollock. At present, the pathway to providing input is through a "grass-roots" approach; the integrative research method employed during SEBSCC included fisheries scientists at the Alaska Fisheries Science Center whose tasks are directed toward status of stocks. Some of these scientists were SEBSCC Principal Investigators and/or members of the Indices and Pribilof Island Working Groups. They were the ones who helped to develop both indices of potential survival of early life histories of pollock and a formal technique to use such indices in stock assessment models. The quantitative use of annual metrics of the physical and biological environment is the next logical step in the progression toward improved forecasts of age-1 recruitment. As the management of fisheries matures toward an ecosystem-based approach, the integrated biophysical

knowledge attained by fisheries scientists during SEBSCC will prove to be an invaluable foundation.

3.6.2 Further development of indices

Based on the results from four workshops, the members of the IWG believe that the following are logical next steps in the development and refinement of indices. These suggestions have been grouped into two categories: indices that are related to changes in strength of a given year class of pollock and an index that may provide guidance regarding interpretation of the annual stock assessment from trawl results. While this later category was not in the original charge to the IWG or a focus of SEBSCC, it is a vital component of fishery management.

Indices for Estimating Recruitment of Age-1 Pollock

- Continue comparisons with other model simulations and observations to provide verification of the Bering Sea model (NEPRIMS).
- Develop a wind index of nutrient supply to the shelf from Bering Canyon.
- Develop a user interface and/or other techniques so the NEPRIMS is more accessible as a tool.
- Examine various indices versus occurrence of northwest and southeast centers of the adult pollock population.
- Extract an index of zooplankton abundance from ECOSYM.
- Develop a history of the time/space occurrence of the roe fishery to help define time/space limits for pollock eggs as initial points for trajectory simulations.
- Develop a similar product for spawning that occurs near Bogoslof Island.
- Use temperature observations from annual trawl surveys to develop an index of the presence of the cold pool and the locations of the inner and middle fronts (i.e., the boundaries of the middle shelf domain) in given years.
- Use temperature observations to create annual distributions of temperature that, in turn, can be used to simulate zooplankton production.

An Index for Interpretation of the Annual Stock Assessment

- Examine the influence of changes in the physical environment (e.g., water temperature, location of fronts) on preferred habitat for pollock, and how variations in these features affect estimates from trawl results.

3.6.3 Concluding remarks

Simulations from the NEPROMS are vital to further development of indices for the Bering Sea ecosystem. Continued verification of simulations (both velocity and water property fields) from this model and improvements to its physics (i.e., inclusion of northward flow through Bering Strait) has the highest priority. The development of a wind-related index of potential nutrient transport shoreward along the Alaskan Peninsula from Bering Canyon can be accomplished independently of the NEPROMS. Comparisons between OSCURS and NEPROMS (Section 3.3.6.2) demonstrate that dynamics other than direct wind forcing are critical throughout most of the water column. Thus, model simulations of the integrated flux through appropriate cross sections would provide a more complete measure of nutrient flux. Model simulations can also be used to establish temperature distributions for a time perhaps more appropriate for making estimates of zooplankton production (May–June) than the July–August data from the trawl survey.

Given the overall importance of NEPROMS simulations to help us understand physical mechanisms and their impact on biota, the utility of this model must be improved. In addition, as techniques and understanding of dynamics improve, this model should be updated to include as much physics as is possible. How can the NEPROMS become a user-friendlier tool? This may take the form of having made and stored average (e.g., daily) water property and velocity field distributions. If these simulations were then coupled with an interactive interface that would allow a naive user to choose particular simulations and then access them in selected time and space domains, then the NEPROMS would permit far more research into indices and questions of how the ecosystem functions than is possible today.